INSTITUTE OF HYDROLOGY

# 1977 UNITED KINGDOM JOINT FLIGHT EXPERIMENT: FINAL REPORT

by

R J GURNEY*, K BLYTH*, J DEJACE†, J R HARDY§, J HUYGEN†, S JAGGER§, M KOHL†, G MARACCI†, J MEGIER†, P REINIGER†, and G TASSONE†

* *Institute of Hydrology*
† *Commission of the European Communities, Joint Research Centre, Ispra, Italy*
§ *University of Reading, UK*

ABSTRACT

A Joint Flight experiment was held in September 1977 in the UK to provide remotely sensed estimates of day- and night-time surface temperature and albedo for use in computer energy balance models for the purposes of estimating soil moisture status and actual evapotranspiration. Sites in Buckinghamshire and Berkshire were overflown, and grassland and bare soil sites were instrumented. The data were quality controlled, including attempts at calibrating the remotely sensed data and a registration of the day-time and nighttime data. Two models were used with the corrected data to estimate evapotranspiration and soil moisture status, with results comparable to other measurements of these quantities.

REPORT NO 85

March 1983

CONTENTS


| | | Page |
|---|---|---|
| 1 | INTRODUCTION | 1 |
| 2 | GENERAL DESCRIPTION OF SITES | 1 |
| | 2.1 Ground data: Grendon Underwood sites | 4 |
| | Bare earth site | 4 |
| | Grassland site | 6 |
| | Conclusions from field measurements at Grendon Underwood | 7 |
| | 2.2 Ground data: Newbury sites | 9 |
| | Plastow Green | 13 |
| | Hannington | 13 |
| | 2.3 Ground data manipulation: Newbury | 13 |
| 3 | AIRCRAFT DATA | 14 |
| | 3.1 Registration of night thermal data over day thermal and visible data | 16 |
| | 3.2 Conclusions | 22 |
| | 3.3 Correction of the scan angle effect on the spectrometric values | 24 |
| 4 | APPLICATIONS OF DIGITAL MODELS | 25 |
| | 4.1 Tergra model sensitivity studies | 25 |
| | Changes in resistance at three different windspeeds | 30 |
| | Effect of changes of one resistance on other resistances | 31 |
| | Effect of uncertainty of parameters on calculated ET values under wet and dry soil conditions | 31 |
| | Effect of uncertainty of parameters on resitances | 32 |
| | Conclusions of the sensitivity analysis | 32 |
| | 4.2 Testing the Tellus model | 32 |
| | 4.3 Creation of look-up tables for point-by-point plotting | 39 |
| 5 | RESULTS - SOIL MOISTURE AND EVAPORATION MAPS | 41 |
| | 5.1 Simulated night temperatures | 41 |
| | 5.2 Thermal inertia and soil moisture | 41 |
| | 5.3 Cumulative daily evaporation | 42 |
| 6 | CONCLUSIONS | 42 |
| | ACKNOWLEDGEMENTS | 43 |
| | REFERENCES | 43 |




# 1 INTRODUCTION

On September 13, 1977, a flight experiment was held in the U.K. in connection with the Tellus Project under the auspices of the Commission of the European Communities, Joint Research Centre, Ispra. The co-operating British institutions were the Institute of Hydrology, Wallingford, and the Universities of Leeds and Reading. The purpose of the experiment was to test the methods to be used to analyze the data from the Heat Capacity Mapping Radiometer, flown on the Explorer-A satellite launched in April 1978. The experiment involved flying a Daedalus DS-1250 multispectral scanner over two areas, at Grendon Underwood, Bucks, and near Newbury, Berks. The organization of the flights has been described by Reiniger (1978) in a companion report. The two areas were equipped with instruments at various sites to measure micrometeorological variables, including the radiation balance and the heat and moisture balances of the layer of the atmosphere closest to the ground and the upper layer of the soil, and the flights over the sites were timed so that two flights took place in a 24-hour period, to coincide with the maximum and minimum diurnal surface temperature.

The aims of the experiment were to test the methods used to analyze data within the Tellus project, and several stages are involved in this analysis. The ground data and the aircraft data have both been prepared into a form suitable for inclusion in digital models, and the performance of two models, the Tergra model (Soer, 1980) and the Tellus model (Rosema *et al.*, 1978) have been discussed. Both models were made available by the Joint Research Centre. The models are used to estimate the actual daily evapotranspiration and soil moisture status, using an energy balance approach. The Tergra model uses one set of overflight data, and the Tellus model requires input data from two flights.

One of the main justifications of the experiment was to provide a data set on which to work, prior to the launch of the satellite. This purpose was amply fulfilled, because there were extreme delays in obtaining any HCMM satellite data, which meant that the only suitable data on which the U.K. investigators were able to work for a considerable time came from the 1977 aircraft experiment. Members of the Joint Research Centre (JRC) also used the data for the same reason.

As briefly described above, there were three stages in the analysis of the data. The ground instruments had to be calibrated, and measurements made on soil samples; the aircraft data had to be converted into a form suitable to be read on each computer, and then converted into equivalent ground temperatures; and the data had to be analyzed using models. These will be discussed in turn for both the Grendon and Newbury sites; the work of all the institutions taking part in the experiment will be described together.

# 2 GENERAL DESCRIPTION OF SITES

Two areas were chosen for the Joint Flight Experiment, one near Grendon Underwood, Bucks, and one near Newbury, Berks. Five sites were delimited, each a square of side 1 km, and instruments were placed in each of these.

The sites are (see also Fig. 1 and 2):

| *Responsible Institute* | *Site* | *Position* |
|---|---|---|
| Institute of Hydrology /JRC | Grendon Underwood | 51°53'10"N 1°00'48"W<br>SP 677 216 |
| Reading University/<br>Leeds University | Crookham | 51°22'30"N 1°14'00"W<br>SU 530 640 |
| | Plastow Green | 51°20'55"N 1°14'00"W<br>SU 530 610 |
| | Hannington | 51°17'45"N 1°13'00"W<br>SU 540 550 |

Grendon Underwood consists of undulating farmland between 60 m and 100 m above mean sea level, with the land being used mainly for cereal crops and pasture and with a field size of up to 15 ha. There are also some small areas of commercial woodland and market gardening. The soils are mainly clay, with some sandstone and alluvium. The area is part of an experimental catchment, that of the River Ray, operated by the Institute of Hydrology. The two sites taken were one grassland site consisting of four fields adjacent to the meteorological station operated by the Institute of Hydrology, on clays of the Evesham Series, and one field of bare ploughed soil, on clays of the Denchworth Series. Adjacent to the bare earth site were several other fields of burnt stubble, from one of which some samples were also taken. At the grassland site, basic instrumentation on the meteorological station was provided by the Institute of Hydrology, with additional instruments and soil samples provided by JRC-Ispra, while the bare soil site was instrumented by the Institute of Hydrology. Other analyses have shown that the Evesham and Denchworth series of clays have very similar mechanical properties, and so may be treated as identical for the purposes of this report.

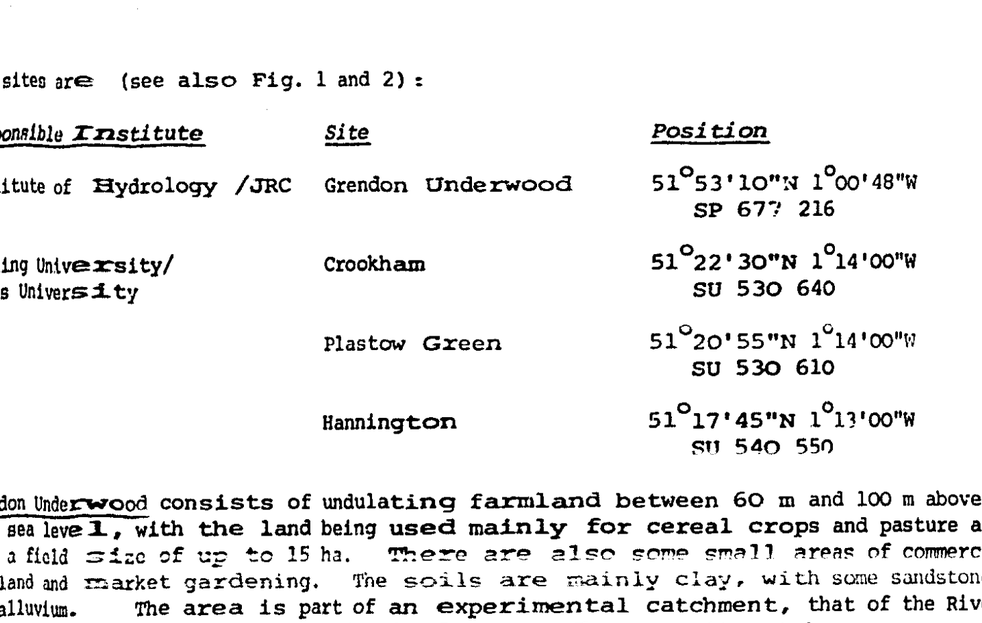


FIGURE 1 Location of test sites near Grendon Underwood, Buckinghamshire



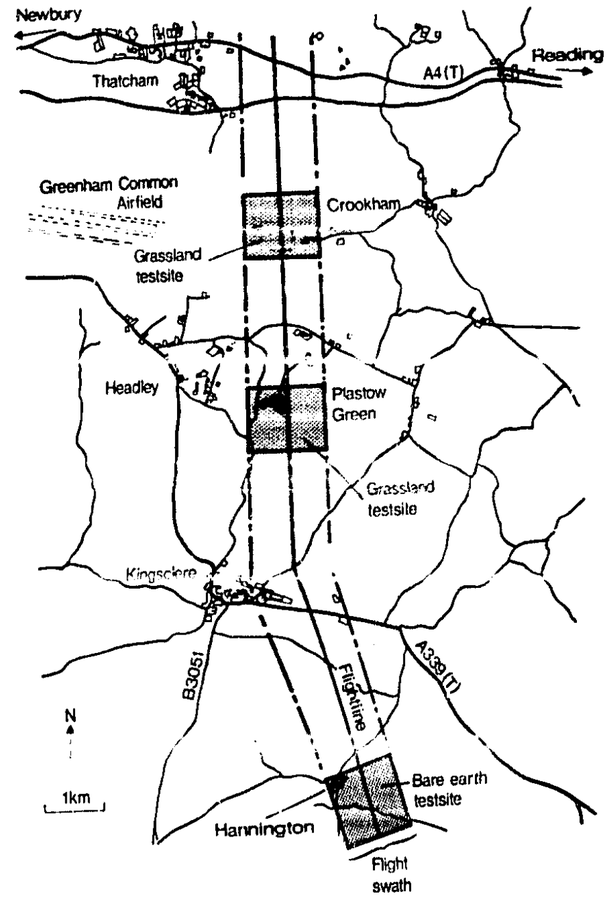


FIGURE 2 Location of test sites near Crookham, Berkshire

Newbury sites consist of undulating land between 70 m and 200 m above mean sea level, with fields up to 12 ha in area. The land is used for cereal crops and pasture, with some commercial woodland and market gardening. Crookham soils are brown earths on terrace gravels of the St. Albans series, and with a water table over 10 m below the surface. The meteorological site was established on permanent pasture, using an automatic weather station provided by the Institute of Hydrology. Maximum and minimum soil thermometers were installed, and soil samples taken; soil moisture content was determined gravimetrically in the laboratory. Plastow Green soils are surface water gley soils overlying loamy drift lying on Wickham Series clays with a water table 1-2 m below the surface. The meteorological station was established on a permanent pasture site, with instrumentation being provided by Reading University. Hannington soils are brown calcareous soils on chalk. The meteorological site was set up on a bare soil site, a ploughed field, using instrumentation provided by Leeds University.

## 2.1 Ground Data: Grendon Underwood sites (see also Table 1)

*Bare Earth Site*

The bare soil site at Grendon Underwood consisted of a field of about 6 ha area, (E in Fig. 3) which had been ploughed and harrowed during the week preceding the overflight, but which retained local surface roughness with an amplitude up to about 20 cm. Fixed instrumentation was installed at three sites, shown in Figure 4, with automatically recording instruments on Site II as specified by Reiniger (1980) - At Sites I and III, manually-read mercury soil thermometers were installed at depths of 5, 10 and 20 cm; shade air temperature was also recorded. Instrumentation at all three sites provided data which was co-incident in time with aircraft overpasses for both day- and night-time overpasses.

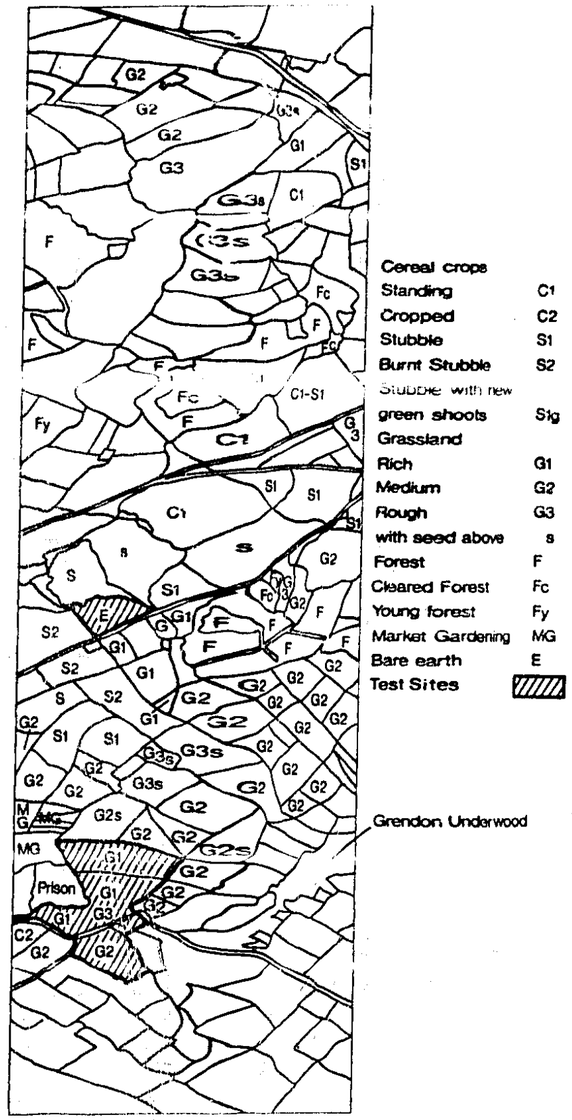


FIGURE 3

Grendon Underwood land-use on 14 September 1977



**TABLE 1 GRENDON UNDERWOOD**

GRENDON UNDERWOOD AUTOMATICALLY RECORDED METEOROLOGICAL AND SOIL DATA

Data recorded on magnetic tape at 5 minute intervals using Microdata logger:

*BARE EARTH SITE (SITE II)*

*Soil temperature* Thermistor temperature probes set at sub-surface (thin soil cover) 2cm below ground level - 5cm below ground level - 20cm below ground level

*Soil albedo* Dual solarimeters set at 1m above ground level sampling ircoming and reflected radiation between 0.3 and 2.5μ.

*GRASSLAND METEOROLOGICAL SITE*

*Automatic weather station* Solar radiation (0.3-2.5μ); Net radiation (0.3-80μ); Wind run; Wind direction; Rainfall; Air temperature and depression.

*Soil heat flux plates* 2 at 5.1cm below ground level - 1 at 10.2cm below ground level - 1 at 20.3cm below ground level

GRENDON UNDERWOOD MANUALLY RECORDED METEOROLOGICAL AND SOIL DATA

| *BARE EARTH SITE* | 05.56am | 13.40pm | 06.00am | 13.47pm | 05.50am | 13.55pm |
|---|---|---|---|---|---|---|
| Soil temperature 5.1cm *a* | 10.0°C | 16.5°C | | | 8.8°C | 17.9°C |
| 5.1cm *b* | | | | | 8.0°C | 19.4°C |
| 10.2cm | 11.5°C | 14.0°C | | | | |
| 20.3cm | 13.4°C | 12.9°C | | | 13.6°C | 13.3°C |
| Earth temperature 50.0cm | | | 12.5°C | 13.6°C | | |
| Shade temperature at 122cm *agl* | 5.5°C | 17.7°C | | | 5.5°C | 17.8°C |
| Wind run at 20cm *agl* | | | 0.2327 | 1.6833 | | |

| *GRASSLAND METEOROLOGICAL SITE* | 06.12am | 13.31pm | Earth temperature | 06.12am | 13.31pm |
|---|---|---|---|---|---|
| Soil temperature 5.1cm | 8.9°C | 21.9°C | 30.5cm | 15.0°C | 14.8°C |
| 10.2cm | 11.8°C | 15.7°C | 61.0cm | 14.9°C | 14.9°C |
| 20.3cm | 13.8°C | 13.8°C | 122.0cm | 14.3°C | 14.3°C |
| Grass temperature | 1.2°C | 23.6°C | | | |
| Grass minimum temperature | -0.2°C | | | | |
| Screen temperature at 122cm *agl* | | | dry bulb | 2.4°C | 16.5°C |
| | | | wet bulb | 2.4°C | 11.6°C |

GRENDON BARE EARTH SITE at 14.15pm on 13.9.77

Location: between soil temperature sites I and II. PRT-5 fitted with 2° optics. Sensor height 75cm *agl*. Variation in recorded temperature with changing look angle and direction.

| (a) Radiometer facing towards sun | Look angle | Surface temperature | |
|---|---|---|---|
| | 0° (vertical) | 24.0°C | |
| | 15° | 22.6°C | |
| | 30° | 34.25°C | |
| | 45° | 28.8°C | |
| | 60° | 28.75°C | |
| | 75° | 25.25°C | |
| | | 27.18°C | Mean temperature |

| (b) Radiometer at constant 45° look angle | Look direction | |
|---|---|---|
| | 0° (facing sun) | 25.70°C |
| | 45°C | 25.75°C |
| | 90°C | 27.25°C |
| | 135° | 31.25°C |
| | 180° | 26.25°C |
| | 225° | 31.50°C |
| | 270° | 28.75°C |
| | 315° | 26.25°C |
| | 360° | 25.25°C |
| | | 25.22°C Mean temperature |

Additional measurements of apparent surface temperature and surface reflection were made using hand-held radiometers (Reiniger, 1980). During the morning preceding and the afternoon following the 1400 overflight, an extensive set of surface soil samples was taken for analysis of water content by weight, in an attempt to identify any local variations in surface soil moisture. Later estimates of soil density enabled volumetric soil moisture content to be calculated. Volumetric sampling of the top layers of the soil was not possible because of the friable nature of the soil; however, eight volumetric samples were taken of the more closely-bound sub-surface layer between 5-20 cm depth. The positions of the measurements and their values are given in Figure 4. Even given that the sampling and analysis methods are different, it is still apparent from Figure 4 that the soil surface was considerably drier than the underlying 15 cm layer.

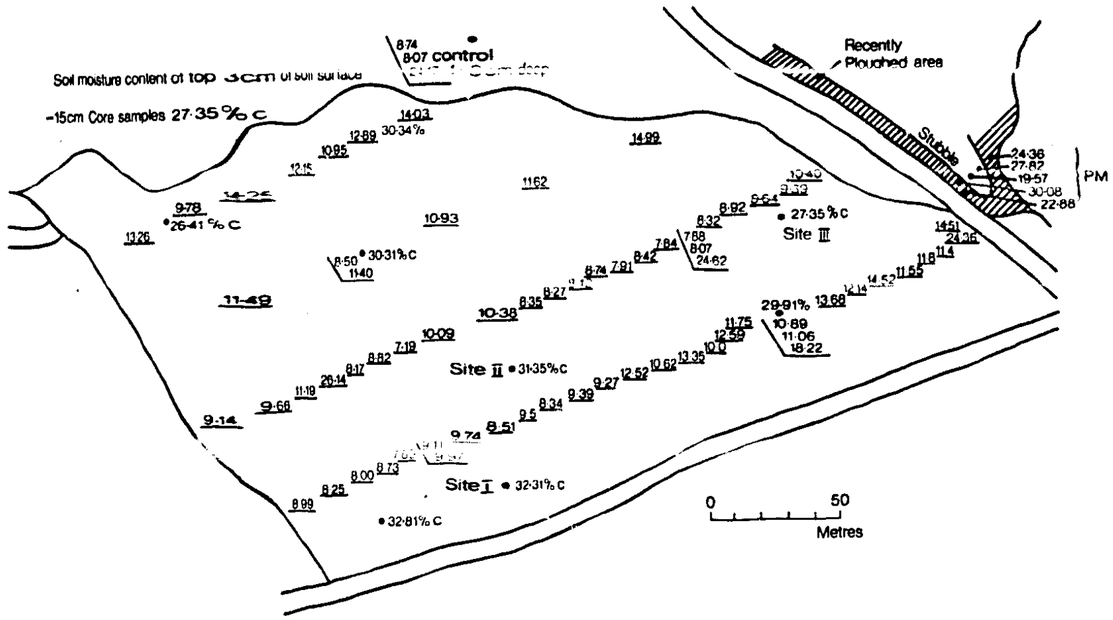


FIGURE 4 Grendon Underwood bare earth site: soil moisture for morning of 13 September 1977

*Grassland Site*

The grassland sites (marked 'G' in Fig. 3) were four fields of various qualities of pasture around the central meteorological site and mobile laboratory, and were instrumented as shown by Reiniger (1980). Nine volumetric samples of the top 2.5 cm of soil were taken, together with three 15 cm core samples. The positions of the measurements and the values obtained are shown in Figure 5. Less variation between surface and subsurface layers was apparent on the grassland than the bare earth sites, as may be expected; generally, the rich grassland was found to be wetter than the rougher and more poorly drained rough grassland.



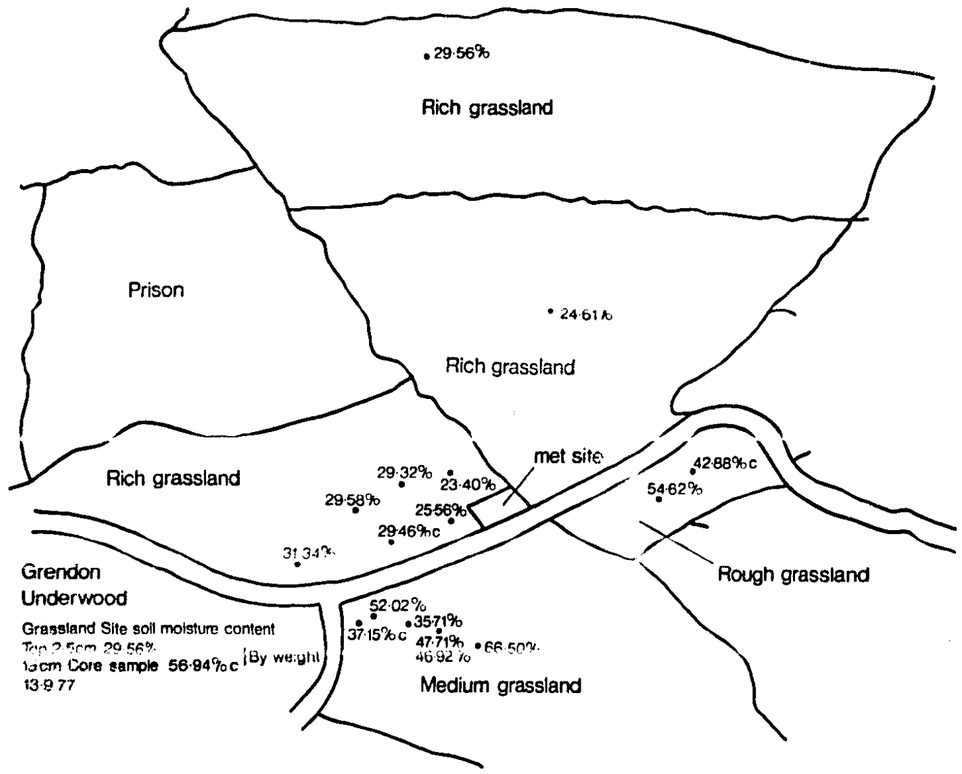


FIGURE 5 Grendon Underwood grassland site: soil moisture for afternoon of 13 September 1977

*Conclusions from Field Measurements at Grendon Underwood*

The physical nature of the bare earth site created considerable problems for the ground measurements both of surface temperature and of soil moisture content, because large differences in both soil moisture and temperature were noted between the peaks and troughs of the rough bare earth surface. Indeed, up to 20°K variations were noted during the afternoon (Figures 6 and 7). In comparison, reliable measurements of both soil moisture content and surface temperature could be made at the grassland sites.

Soil moisture content even near the surface may be assumed to vary only slowly over a period of a few hours, and so adequate estimates of spatial variations may be made. However, this was difficult to achieve for surface temperatures, for comparison with the aircraft scanner data, because of the rapid changes occurring over time, particularly during the afternoon overpass. The co-incidence of aircraft and ground measurements is therefore crucial in order to give sensible results.

Some of the instrumentation was shown not to be very satisfactory. The position of instruments should either be surveyed in to locate their positions on aircraft data, or else ground markers should be laid out. Event marks should also be recorded on portable radiometer recorders to mark the time of each overpass, and

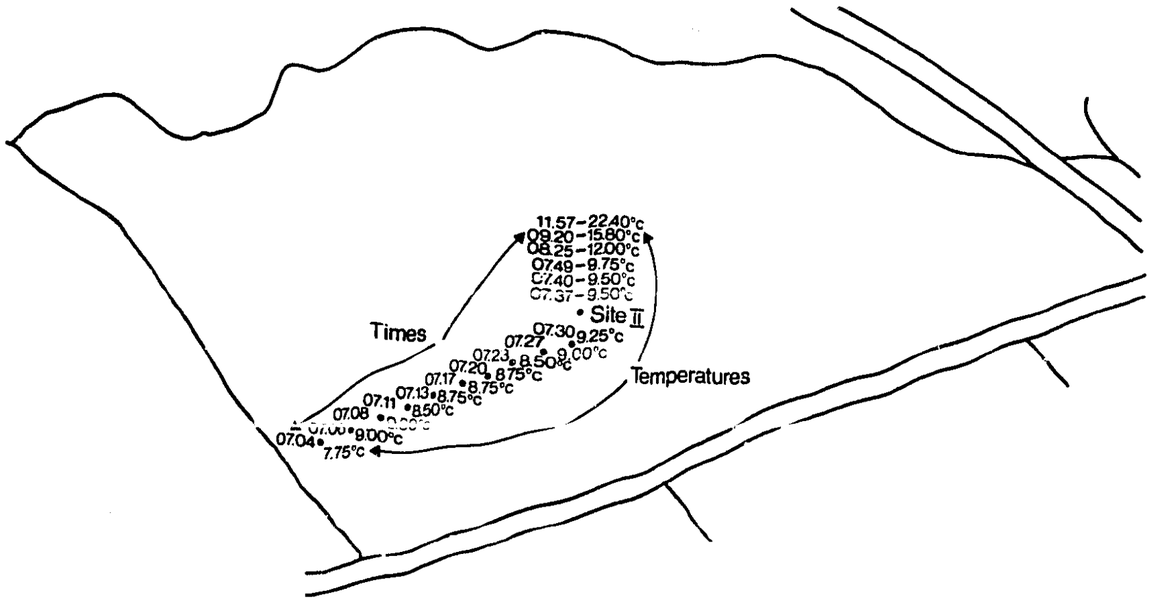


FIGURE 6 Grendon Underwood bare earth site: surface temperature for morning flight on 13 September 1977 using Barnes PRT-5 radiometer with 2° f.o.v.

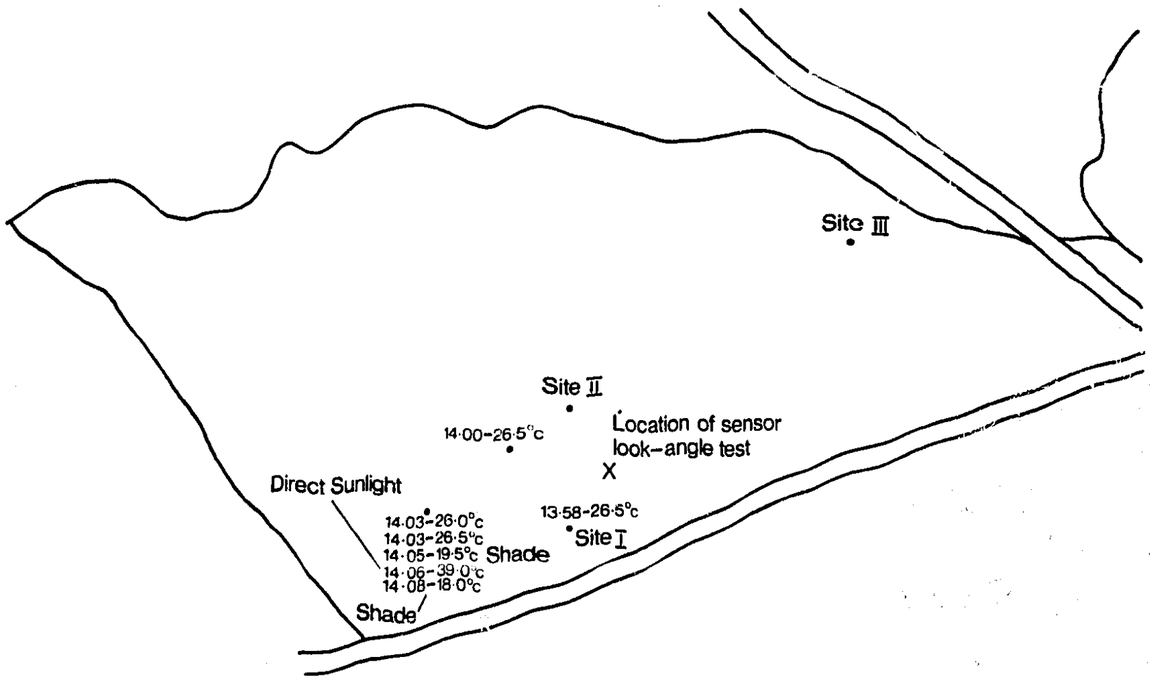


FIGURE 7 Grendon Underwood bare earth site: surface temperature for afternoon flight on 13 September 1977 using Barnes PRT-5 radiometer with 2° f.o.v.



radiometers should be mounted vertically, several metres above the ground and with wide-angle optics to give a field of view comparable with the pixel size of an aircraft-mounted scanner.

Some of the data are reproduced to give an indication of what was recorded, and of the size of the quantities measured.

## 2.2 Ground Data: Newbury Sites

The major part of the equipment was attached to automatically recording data loggers and these were continuously run for the 24 hour period embracing the two aircraft flights. The data collected are summarized in Tables 2-5 which show the variation of the measured parameters throughout this period at hourly intervals only.

Additional equipment was installed at the Plastow Green site to monitor the Bowen ratio and thus provide an independent check on the use of thermal infrared data as a measure of the evaporative flux.

Gravimetric soil moisture content was obtained. Later measurements of the soil bulk density at one site permitted calculation of the volumetric water content.

TABLE 2 CROOKHAM

| Time (hrs) | Incoming Solar Radiation ( $Wm^{-2}$) | Net Radiation (Total) ($Wm^{-2}$) | Air Temperature (°C) | Vapour Pressure (mb) | Wind Speed ($ms^{-1}$) |
|---|---|---|---|---|---|
| 0 | 0 | -68.6 | 8.5 | 10.88 | 1.0 |
| 1 | 0 | -56.3 | 8.2 | 10.29 | 0 |
| 2 | 0 | -50.5 | 7.1 | 9.86 | 0 |
| 3 | 0 | -44.7 | 6.9 | 9.47 | 0 |
| 4 | 0 | -38.8 | 6.3 | 9.27 | 0 |
| 5 | 0 | -33.0 | 6.3 | 9.27 | 0 |
| 6 | 25.1 | -9.7 | 5.7 | 8.68 | 0 |
| 7 | 158.7 | 54.4 | 8.4 | 10.20 | 0 |
| 8 | 316.0 | 193.2 | 10.7 | 12.70 | 0.3 |
| 9 | 374.3 | 238.8 | 12.9 | 15.60 | 2.3 |
| 10 | 490.7 | 331.6 | 13.7 | 15.15 | 3.0 |
| 11 | 565.6 | 383.8 | 14.3 | 15.60 | 2.6 |
| 12 | 640.4 | 436.0 | 15.5 | 16.08 | 1.6 |
| 13 | 588.1 | 392.8 | 15.6 | 15.00 | 2.3 |
| 14 | 546.6 | 358.2 | 16.6 | 16.96 | 1.6 |
| 15 | 422.4 | 265.7 | 16.4 | 16.76 | 1.3 |
| 16 | 283.6 | 161.8 | 16.2 | 16.38 | 1.3 |
| 17 | 107.7 | 5.8 | 15.4 | 16.58 | 0 |
| 18 | 8.3 | -51.2 | 13.9 | 15.40 | 0 |
| 19 | 0 | -57.0 | 11.5 | 13.24 | 0 |
| 20 | 0 | -52.8 | 10.7 | 12.90 | 0 |
| 21 | 0 | -57.0 | 9.5 | 12.40 | 0 |
| 22 | 0 | -56.3 | 6.7 | 9.24 | 0 |
| 23 | 0 | -50.5 | 7.1 | 9.16 | 0 |
| 24 | 0 | -50.5 | 5.9 | 9.07 | 0 |

**TABLE 3** **PLASTOW GREEN**

| Time (hrs) | Wind Run ms-1 | Incoming Solar Radiation ($Wm^{-2}$) | Outgoing Short Wave Radiation ($Wm^{-2}$) | Net Radiation ($Wm^{-2}$) | Soil Heat flux ($Wm^{-2}$) Surface | 10 cm | Soil Temperatures °C 5 | 10 | 25 | 60 cm |
|---|---|---|---|---|---|---|---|---|---|---|
| 1 | 0 | 0 | 0.3 | -57.9 | -.03 | -.01 | 12.6 | 13.4 | 14.5 | 14.1 |
| 2 | 0 | 0 | 0.3 | -55.3 | -.04 | -.02 | 12.1 | 12.9 | 14.2 | 14.1 |
| 3 | 0 | 0 | 0.3 | -46.4 | -.04 | -.02 | 11.9 | 12.7 | 14.1 | 14.1 |
| 4 | 0 | 0 | 0.3 | -32.0 | -.04 | -.02 | 11.5 | 12.3 | 13.7 | 14.1 |
| 5 | 0 | 0 | 0.3 | -28.5 | -.04 | -.02 | 11.1 | 12.1 | 13.4 | 14.1 |
| 6 | 0 | 0 | 0.6 | -23.5 | -.04 | -.02 | 10.7 | 11.8 | 13.4 | 14.1 |
| 7 | 0 | 7.2 | 2.7 | -28.4 | -.04 | -.02 | 10.4 | 11.4 | 13.2 | 14.1 |
| 8 | 0 | 114.1 | 22.2 | +7.9 | -.03 | -.01 | 10.4 | 11.4 | 13.2 | 14.1 |
| 9 | 1.8 | 306.8 | 50.4 | +90.1 | -.01 | -.01 | 10.5 | 11.2 | 13.0 | 14.1 |
| 10 | 2.5 | 413.6 | 78.9 | +186.3 | +.01 | -.01 | 11.0 | 11.3 | 12.9 | 14.1 |
| 11 | 2.0 | 568.3 | 103.2 | +275.2 | +.01 | -.01 | 12.2 | 11.8 | 12.8 | 14.1 |
| 12 | 1.4 | 556.4 | 98.9 | +283.5 | +.04 | +.01 | 13.8 | 12.5 | 12.9 | 14.1 |
| 13 | 1.9 | 619.1 | 124.3 | +236.9 | +.06 | +.02 | 14.8 | 13.4 | 13.1 | 14.1 |
| 14 | 1.2 | 554.4 | 119.8 | +320.8 | +.07 | +.02 | 16.0 | 14.3 | 13.4 | 14.1 |
| 15 | 1.0 | 395.5 | 120.8 | +344.2 | +.07 | +.03 | 18.8 | 15.2 | 13.8 | 14.1 |
| 16 | 1.0 | 614.5 | 106.0 | +292.9 | +.05 | +.03 | 17.2 | 16.1 | 14.2 | 14.1 |
| 17 | 0 | 460.7 | 81.2 | +198.7 | +.04 | +.03 | 17.1 | 16.5 | 14.5 | 14.0 |
| 18 | 0 | 287.0 | 53.5 | +89.9 | 0 | +.02 | 16.6 | 16.7 | 14.9 | 14.0 |
| 19 | 0 | 89.7 | 14.9 | +25.3 | 0 | +.01 | 16.1 | 16.5 | 15.0 | 13.9 |
| 20 | 0 | 4.6 | 1.8 | 0 | 0 | 0 | 15.4 | 16.0 | 15.0 | 13.9 |
| 21 | 0 | 0 | 0.3 | -55.9 | 0 | 0 | 14.6 | 15.4 | 15.0 | 13.9 |
| 22 | 0 | 0 | 0.3 | -55.2 | 0 | 0 | 14.1 | 14.6 | 15.0 | 13.9 |
| 23 | 0 | 0 | 0 | -56.7 | 0 | 0 | 13.7 | 14.2 | 14.8 | 13.9 |
| 24 | 0 | 0 | 0 | -56.9 | 0 | 0 | 13.5 | 13.9 | 14.8 | 13.9 |
| | | | | | | | 13.2 | 13.6 | 14.7 | 13.9 |

TABLE 4 HANNINGTON

| Time (hrs) | Incoming Solar Radiation ($Wm^{-2}$) | Outgoing Short Wave Radiation ($Wm^{-2}$) | Net Radiation ($Wm^{-2}$) | Air Temperature °C | Vapour Pressure (mb) | Wind Speed at 2 m | Wind Speed at 0.10 m | Soil Temperatures °C 1 | 2 | 5 | 10 | 20 cm | Infrared Surface Temperature |
|---|---|---|---|---|---|---|---|---|---|---|---|---|---|
| 0 | 0 | 0 | -80.1 | 8.2 | 10.2 | 0 | 0 | 5.0 | 5.3 | 14.7 | 14.4 | 14.1 | |
| 1 | 0 | 0 | -74.2 | 8.5 | 10.3 | 0.1 | 0 | 4.9 | 5.2 | 14.7 | 14.1 | 14.1 | 6.0 |
| 2 | 0 | 0 | -56.3 | 8.3 | 9.8 | 0 | 0 | 5.0 | 5.2 | 14.7 | 13.9 | 14.0 | 5.5 |
| 3 | 0 | 0 | -48.7 | 8.4 | 9.5 | 0 | 0 | 4.7 | 5.0 | 14.4 | 13.1 | 13.9 | 5.0 |
| 4 | 0 | 0 | -33.0 | 8.3 | 9.5 | 0 | 0 | 4.1 | 4.6 | 14.2 | 13.0 | 13.6 | 4.8 |
| 5 | 0 | 0 | -38.3 | 7.7 | 9.3 | 0 | 0 | 4.1 | 4.4 | 14.1 | 12.8 | 13.3 | 4.5 |
| 6 | 0 | 0 | -34.6 | 7.1 | 9.0 | 0 | 0 | 3.6 | 4.3 | 14.0 | 13.0 | 13.2 | 4.2 |
| 7 | 16.2 | 8.1 | -27.3 | 6.4 | 8.4 | 0.1 | 0.1 | 3.6 | 4.2 | 14.0 | 12.8 | 13.2 | 8.0 |
| 8 | 105.4 | 32.4 | +9.2 | 8.7 | 10.2 | 0.2 | 0.1 | 5.1 | 4.7 | 14.2 | 12.8 | 13.2 | 11.0 |
| 9 | 235.2 | 48.7 | +72.1 | 12.3 | 12.1 | 1.7 | 1.4 | 10.0 | 5.1 | 14.3 | 12.1 | 13.2 | 15.6 |
| 10 | 296.1 | 56.8 | +80.1 | 14.3 | 14.5 | 2.2 | 2.2 | 10.1 | 6.0 | 14.5 | 12.2 | 13.2 | 15.8 |
| 11 | 381.2 | 73.0 | +140.5 | 16.8 | 17.9 | 1.9 | 2.0 | 16.0 | 7.5 | 6.9 | 12.3 | 13.2 | 24.3 |
| 12 | 433.9 | 77.6 | +210.3 | 16.9 | 15.3 | 1.9 | 1.8 | 21.1 | 8.8 | 15.5 | 12.2 | 13.2 | 29.2 |
| 13 | 507.7 | 101.4 | +225.6 | 18.6 | 16.6 | 1.9 | 1.9 | 25.0 | 13.4 | 15.9 | 13.6 | 13.2 | 29.6 |
| 14 | 539.3 | 93.4 | +280.9 | 17.7 | 15.2 | 1.7 | 1.6 | 25.8 | 14.6 | 16.3 | 14.6 | 13.3 | 33.5 |
| 15 | 502.8 | 89.2 | +310.6 | 17.5 | 15.1 | 1.2 | 1.1 | 26.7 | 16.0 | 16.6 | 15.2 | 13.5 | 24.4 |
| 16 | 417.7 | 72.1 | +296.7 | 16.6 | 14.3 | 1.0 | 1.2 | 24.5 | 16.5 | 16.8 | 15.8 | 13.6 | 23.8 |
| 17 | 292.0 | 52.7 | +150.6 | 16.9 | 14.6 | 1.0 | 0.9 | 20.5 | 17.4 | 16.7 | 16.2 | 13.8 | 18.6 |
| 18 | 146.0 | 28.4 | +140.7 | 15.9 | 14.1 | 0.8 | 0.6 | 15.0 | 17.2 | 16.7 | 16.4 | 13.8 | 16.0 |
| 19 | 16.2 | 4.1 | +6.2 | 14.1 | 13.9 | 0 | 0 | 10.2 | 13.3 | 16.5 | 16.3 | 14.0 | 12.2 |
| 20 | 0 | 0 | +4.2 | 11.9 | 11.3 | 0 | 0 | 8.2 | 10.9 | 16.0 | 15.9 | 14.0 | 16.0 |
| 21 | 0 | 0 | -60.6 | 10.1 | 10.3 | 0 | 0 | 6.4 | 7.1 | 15.7 | 15.5 | 14.0 | 9.8 |
| 22 | 0 | 0 | -70.3 | 9.2 | 10.1 | 0 | 0 | 4.9 | 6.3 | 15.6 | 15.3 | 13.9 | 9.2 |
| 23 | 0 | 0 | -71.6 | 9.1 | 10.0 | 0 | 0 | 4.9 | 5.7 | 15.5 | 15.1 | 13.9 | 8.1 |
| 24 | 0 | 0 | -79.8 | 8.7 | 9.8 | 0 | 0 | 4.9 | 5.4 | 15.5 | 14.7 | 13.9 | 6.7 |

TABLE 5

**SOIL MOISTURE CONTENT (%)**

| Depth | 0600 hours | 1400 |
|---|---|---|
| Plastow Green | | |
| Surface, cm | 16.9 ± 2.8 | 15.9 ± 1.3 |
| 5 | 17.5 ± 1.6 | 17.3 ± 0.8 |
| 10 | 17.4 ± 0.7 | 16.5 ± 2.5 |
| 20 | 18.1 ± 1.4 | 16.3 ± 0.5 |
| Volumetric | 16.1 ± 2.6 | 16.4 ± 2.0 |
| Hannington | | |
| Surface, cm | 5.9 ± 1.0 | 5.1 ± 0.7 |
| 5 | 19.8 ± 2.3 | 18.5 ± 4.9 |
| 10 | 20.0 ± 1.5 | 22.0 ± 1.7 |
| 20 | 22.7 ± 1.2 | 23.1 ± 2.9 |



*Plastow Green*

Sampling Scheme. Five sampling points were chosen. Four were located in directions NE, SE, SW and NW of the point of meteorological observation, and at 10 m distant. They are denoted by their direction from the meteorological mast. The fifth was as close to the meteorological site as practical. At each sampling point soil was taken from four depths, viz; surface, 5, 10 and 20 cm, and twice during the day - 06.00 and 1400 hours. Figures in brackets refer to volumetric water content.

*Hannington*

Sampling scheme. The Plastow Green sampling scheme was followed for points close to the site of meteorological observation. However, additional points were chosen at larger distances from the meteorological mast.

## 2.3 Ground Data Manipulation: Newbury

The ground data have been treated in several ways both to assess their accuracy and to compute parameters not amenable to field determination.

At the time of the experiment only gravimetric soil samples were obtained. Later experience revealed that volumetric sampling was necessary to facilitate comparison of aircraft-derived soil moistures and those measured on the ground. A further programme of sampling was then begun to determine the porosity of soils at the sites. It is assumed in this procedure that there is little variation with time of the porosity, when the soil remains in the same state. Thus, heat capacity, thermal conductivity and thermal inertia depend on the volumetric water, air and mineral content of the soil and can be computed if these are known.

Various meteorological parameters permitted correlation with airborne measurements. At one site a Barnes Instatherm Infra Red thermometer was positioned so as to monitor the infra red emission temperature of the surface. This instrument first proved unsatisfactory in operation. Its optics provide a $2^{\circ}$ field of view only and consequently, if it is not to view merely anomalies in the soil surface, it must be installed at a considerable height. This introduces the problem of controlled temperature environment. Each temperature reading requires a correction for the case temperature and thus some external means must be provided for this.

At two sites a pair of solarimeters placed back to back provide an integrated measurement of the short wave albedo in the wavelength range 0.3 to 2.5 μm.

Such data have been used for input to the numerical models and can be compared to albedos measured by the visible channels of the multispectral scanner (MSS). A procedure for integrating separate MSS channel albedos to provide a total value over the entire wavelength range of the instrument has also been done, and results agree well with ground measurements.

Measurements of the Bowen ratio β can yield information on the behaviour of evaporation. This parameter was computed from the site set on stubble at Plastow Green. At any instant, the latent heat flux L.E can be computed from knowledge of this parameter, the soil heat flux G and the net radiation $R_N$ using the relation

$$L.E = \frac{R_N - G}{1 + \beta}$$

From this it is a simple matter to calculate the cumulative daily value for the evaporation.

An examination of soil heat flux data at the station where flux plates were installed showed they functioned unsatisfactorily. Using measured soil temperatures and a realistic thermal conductivity of 1.7 $Wm^{-1}\ ^oC^{-1}$ in the heat conduction equation indicates that at 1200 hours the measured soil heat flux at 10 cm should be ~ 15 $Wm^{-2}$. That measured with the flux plate was .01 $Wm^{-2}$, so clearly such data must be disregarded.

An assessment of the accuracy of measurement of the radiation components at a station can be made by correlating measured net radiation with that computed from long and short wave radiation components. Net radiation is given by

$$R_N = (1 - \alpha_s)\ R_S + (1 - \alpha_L)\ R_L - \varepsilon\sigma\ T_c^4$$

where $R_S$ and $R_L$ are short- and long-wave radiation inputs

$\alpha_s$ and $\alpha_L$ are short- and longwave reflection coefficients

$\varepsilon$ is the surface emission coefficient

$\sigma$ is the Stefan-Boltzmann constant

$T_c$ is the surface temperature

This can be written as

$$R_N = (1 - \alpha_s)\ R_S + \varepsilon\sigma\ (T_a^4 - T_c^4)$$

since $\varepsilon_a + \alpha_L = 1$, $\varepsilon_a = \varepsilon_c = \varepsilon$

and so $R_L = \varepsilon\sigma\ T_a^4$

where $T_a$ is the air temperature.

Such an analysis of ground data at the sites provided a suitable positive check on the data quality.

## 3 AIRCRAFT DATA

Several types of data from the aircraft were made available. Only a few hours after the experimental flights, quick-look thermal images of the entire swath were made available. Such imagery enabled a rigorous and accurate land-use survey to be made of the whole area. The images were used as maps of different tonal areas, each of which was associated with a different land use cover type.

The final products of the aircraft flight were of three types. False colour infra-red photography was supplied in a 22 cm format, and were used to check the land use maps where necessary. Data from the multispectral scanner were obtained in two forms. For the night-time flight, thermal data only were available. Day-



time observations comprised both thermal and reflected solar radiation divided into ten channels, the wave bands of each channel being given in Table 6. Work has proceeded almost exclusively with the scanner data contained on computer compatible tapes, which were obtained when the analogue tape on which the data from the scanner were recorded were digitized to 8 bits (i.e. 256 quantization levels).

TABLE 6 WAVELENGTH AND WIDTH OF BANDS OF EXOTECH-100A AND DAEDALUS DS-1250

| EXOTECH 100A band (nm) | Δλ (nm) | DAEDALUS DS-1250 band (nm) | Δλ (nm) |
|---|---|---|---|
| 496 - 596 | 96 | 500 - 550 | 50 |
| | | 550 - 600 | 50 |
| 580 - 706 | 126 | 600 - 650 | 50 |
| | | 650 - 690 | 40 |
| 687 - 819 | 132 | 700 - 790 | 90 |
| 767 - 974 | 207 | 800 - 890 | 90 |
| | | 920 - 1100 | 180 |

There were some problems adapting the tape data to be read at each institute or university. JRC used byte-based computers and so had no problems with tape translations, but the Institute of Hydrology had a Univac 1108 machine, which is a word-based machine with a word length of 36 bits, and Leed University and Reading University both used word-based machines with a 24-bit word length (I.C.L. 1906A and 1904S respectively). The approach adopted at the U.K. sites is exemplified by Gurney and Templeman (1982), who describe remotely sensed data handling on the Univac 1108 of the Institute of Hydrology. 4 bytes off the tape are stored in each 36-bit Univac word, one byte in each quarter word with the leading bit zero-filled. A function is called to extract the values in each byte and place them right-justified into integer whole words as required. At Reading and Leeds Universities, three bytes of data on the tape have been combined into each ICL word in buffer storage, and then functions called to place each byte right-justified in a whole 24-bit integer word as required. At Reading and Leeds Universities, also, sections of the data which are most heavily used, particularly those around each ground measurement site, have been translated into files held on disc on the computer, to reduce processing time. This has not been done at the Institute of Hydrology to the same extent because of the lower tape loading overheads at that site. Each tape also contained at least one header block of information, which was encoded partly in binary, partly in ASCII, and partly in EBCDIC. At all the U.K. computer sites these data were translated to ASCII code using look-up tables before being written out, to ease handling. It is recommended that in future flights the headers be simplified to include only one type of code to reduce handling difficulties.

All the data which have been examined are of very high quality, with no missing lines or pixels being apparent. However, the very large amounts of data collected led to the investigation of some techniques designed to aid location of areas of interest, in particular, methods of edge detection. Several edge detectors described by Rosenfeld and Kak (1976) were used to try to locate the field boundaries to tie the aircraft and ground data together and to locate trees and other tall vegetation. Two gradient measures were used at the Institute of Hydrology on the Grendon data, the first differences in two dimensions and the digital Laplacian. Neither were found to be very satisfactory because of the large spatial variations present within many fields and because of the width of many edges in terms of the number of pixels occupied by the edge, as the scanner gave very good spatial

resolution. An eyeball approach was thus adopted, using colour displays where necessary. The Institute of Hydrology have been able to use a colour display belonging to the U.K. Atomic Energy Research Establishment for this purpose, taking off the positions of field boundaries and roads using a cursor and joystick.

In order to use the aircraft data, these must be geometrically and radiometrically corrected; the corrections will be described in turn.

### 3.1 Registration of Night Thermal Data Over Day Thermal and Visible Data

Day thermal and visible data are automatically registered for they were acquired during the same flight through the same instrument optics and with the same resolution, 2.5 m at 1000 m altitude. Night thermal data acquired during a previous flight have the same resolution but they must be superposed to day data.

The geometric errors are modelled using bivariate polynomials as mapping functions. A pixel with coordinates (x, y), given by the line and column position in the day data, is thus the transformed element from a pixel with coordinates (u, v) in the night data such that:

$$u = u(x, y) = \sum_{p=0}^{N} \sum_{q=0}^{N-p} a_{pq} x^p y^q$$

$$v = v(x, y) = \sum_{p=0}^{N} \sum_{q=0}^{N-p} b_{pq} x^p y^q$$

where u and v are calculated from x and y.

In the present case second order polynomials were chosen. The method uses ground control points which are common to day and night data to determine the $a_{pq}$ and $b_{pq}$ parameters by least squares fitting. The fitting of the ground control points is performed in the untransformed grid (night data) rather than in the transformed grid (day data), as would seem more natural. The latter solution would require the expression of the (x, y) coordinates as a function of the (u, v) coordinates, i.e. to reverse the preceding expressions. The calculated (u, v) coordinates will not generally be integer and the nearest neighbour rule is applied to determine the pixel radiometric value. This simple procedure has been preferred in the present case to interpolation or convolution methods because for high resolution data errors are not critical and much computer time is saved.

As the complete strip of data is rather long (more than 4000 lines of 672 pixels), the registration is made for successive blocks of 672 x 300 points with a 50% overlap; 12 to 20 control points by block determine the respective pair of transformation polynomials. Discontinuities between blocks are avoided by combining with variable weights the coefficients of the polynomials referring to two successive blocks. As the line of data processed moves from the centre of the first block to the centre of the second block, the weights relative to the first pair of polynomials are changed line by line from 1 to 0, the reverse being done for the second pair. The process is then repeated with the second and third blocks and so on.

The results obtained are displayed in Figures 8-16. The average registration error between ground control points was found to be 2-3 pixels with minimum 0 and maximum 7 pixels.



FIGURE 8

Mapped night temperatures, original data. Range of variation 0°C - 18°C (radiative values)

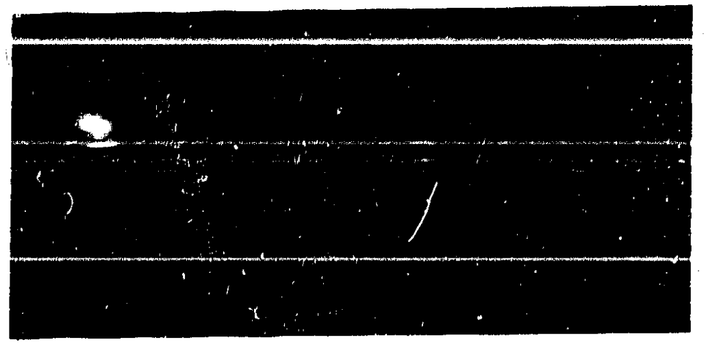

FIGURE 9

Mapped night temperatures. Data geometrically corrected. The transformation is visible through the grid deformation.

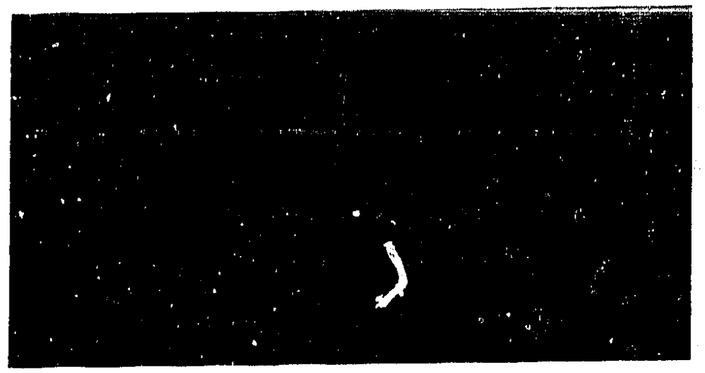

FIGURE 10

Mapped day temperature. Range of variation 8°C - 44°C (radiative values)

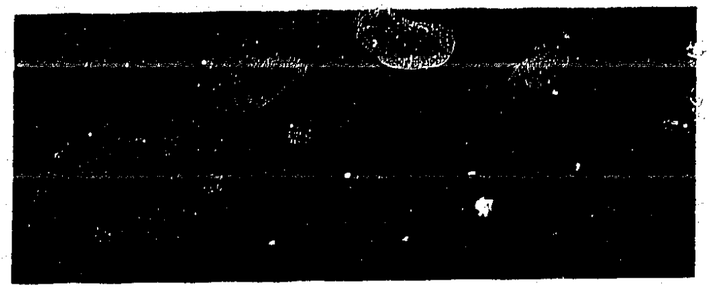

FIGURE 11

Mapped albedo values. Range of variation 0.C2 - 0.20 in the investigated fields.

FIGURE 12

Temperature differences (Td - Tn) mapped in 6 grey levels.

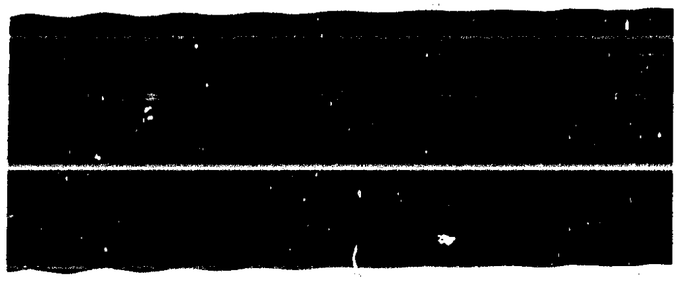

FIGURE 13

Apparent thermal inertia mapped in 6 grey levels.

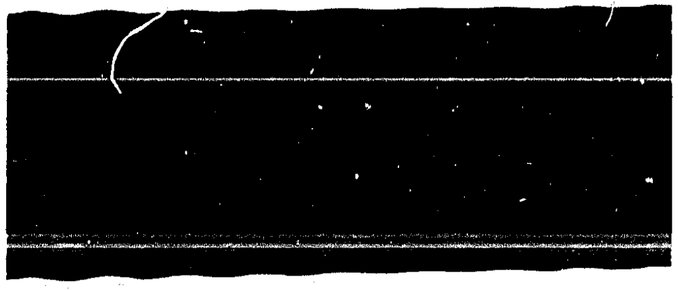

FIGURE 14

Cumulative daily evaporation calculated by Tellus and mapped in 5 grey levels (mm). 1: bare soil; 2: stubbles; 3: burnt & unburnt stubbles; 4 stubbles with green shoots; 5: stubbles & cropped cereals.

FIGURE 15

Thermal inertia and soil moisture calculated by Tellus and mapped in 6 grey levels.

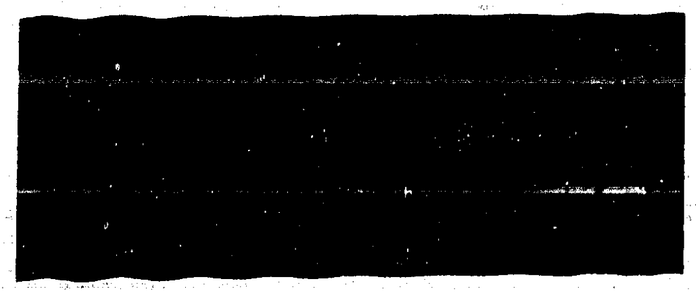

FIGURE 16

Difference between Fig. 15 and Fig. 13 mapped in 5 grey levels.



The data must also be radiometrically corrected, the thermal channels then giving estimated surface temperatures and the nine visible channels albedo, for use in the models. This involves both converting the digitized signal from the radiometer into raw temperatures and radiances, and also correcting for atmospheric transmission and soil surface emissivity. The thermal data contains two calibration sources on the scanner, which correspond to the upper and lower limits over which temperatures are digitized. Assuming a linear relationship between quantization and emission, an estimate of temperature may be made easily. However, a map of surface temperatures may be computationally expensive where large amounts of data are used, and so a look-up table may be generated and used. Estimates of both the incoming long-wave radiation and the infra-red emissivity of the surface were necessary for estimating the surface temperatures; these were obtained either from measurements for incoming long-wave radiation or partly from measurements and partly from published data for infra-red emissivity. Future experiments should include many more such measurements.

Corrections to the aircraft data must be made for atmospheric absorption, which is related to scan angle. JRC corrected for scan angle by fitting a polynomial along each scan line, using linear least squares, and then correcting the data using these functions to relate the radiance at the edge of the scan line to the radiance at the nadir point, and correcting the former to the latter. The differences between temperatures estimated from the radiometers mounted on the aircraft and on the ground are very small, and so no corrections for atmospheric effects were made to the thermal channels of the aircraft scanner data. (See Table 7). Some measurements made by JRC using a PRT-5 hand-held radiometer gave rather anomalous readings, up to 7K different from the estimated scanner values, but these were considered to be caused by power supply problems from the portable batteries.

The incoming hemispherical irradiance at the Grendon Underwood grassland site was measured continuously with an EXOTECH-100A radiometer from 12.30 hours GMT, half an hour before the flight, to 13.30 hours GMT, half an hour after the flight.

At the same time, the radiance reflected toward zenith was measured 2 m above the ground with a second EXOTECH radiometer, in four different fields along the flight line. The FOV of the instrument was $15^{o}$. The fields were:

- ploughed bare soil
- grassland (meadow)
- burnt stubble
- stubble.

All measurements were referred to flight time (13.00 GMT) when at Grendon the sun elevation ($h^{o}$) was $40^{o}39'$. During the flight, measurements of the atmospheric parameters Lp (path radiance) and $\tau$ (transmittance) were performed from the ground using the technique of Rogers and Peacock (1973) which had already been tested at the Joint Research Centre (1975).

In order to compare data measured on the ground with data from the airborne multispectral scanner, it was necessary to take into account the difference in the spectral bands of our field radiometer and those of the airborne Daedalus scanner. The spectral bands of the two instruments are given in Table 6. Simplifying assumptions concerning the spectrum of the hemispherical incoming irradiance, as well as the spectral reflectance of the vegetation were made to derive values of

TABLE 7 COMPARISON OF SURFACE TEMPERATURE MEASURED FROM THE AIRCRAFT AND ON THE GROUND (°C)

| Bare Soil | Day | Night | Albedo | Size Pixels | m² |
|---|---|---|---|---|---|
| Measured (S.W.) | 23.5 ± 1.5 | 4.0 ± 0.6 | | | |
| Measured (S.E.) | 23.9 ± 2.2 | 2.4 ± 0.7 | | | |
| Aircraft (S.W.) | 26.2 ± 0.6 | 4.2 ± 0.2 | 0.10 | 314 | 2000 |
| | 26.1 ± 0.6 | 4.1 ± 0.2 | 0.10 | 815 | 5100 |
| (S.E.) | 27.0 ± 0.8 | 3.8 ± 0.2 | 0.09 | 198 | 1200 m² |
| Whole field | 26.0 ± 0.9 | 4.1 ± 0.3 | 0.09 | 9494 | 6 km |
| Road-Flight Line | | | | | |
| Measured | 29.0 ± 0.7 | 7.2 ± 0.7 | | | |
| Aircraft | 25.1 | 6.5 | | | |
| Dirt Road | | | | | |
| Measured | 26.4 | 5.8 | | | |
| Aircraft | 27.6 | 5.2 | | | |
| Road Edge of Wood | | | | | |
| Measured | | 6.38 | | | |
| Aircraft | | 6.20 | | | |
| Burnt Stubble | | | | | |
| Measured | 27.9 ± 0.8 | 4.2 ± 0.4 | | | |
| Aircraft | 28.0 ± 0.6 | 5.1 ± 0.2 | | | |
| Stubble | | | | | |
| Measured | 21.6 ± 1.7 | 5.5 ± 0.4 | | | |
| Aircraft | 24.5 ± 1.0 | 5.7 ± 0.2 | | | |
| Grassland | | | | | |
| Measured | 20.0 0.9 | 2.7 0.5 | | | |
| Aircraft | 20.4 1.0 | 2.8 0.4 | | 9262 | 17800 m² |
| (diff. field & time) | | | | | |
| + hedges | 20.1 1.7 | 2.9 0.7 | | 12918 | 80700 m² |
| Wood | | | | | |
| Aircraft | 14.6 0.8 | 5.6 | | 2463 | 15400 m² |

| Air Temperature | 12 GHT | 13 GMT | 0.4 GMT | 5 GMT |
|---|---|---|---|---|
| | 15.6 | 17.0 | 2.7 | 2.3 |



the incoming irradiance and of the reflected radiance in the Daedalus bands, from values measured in the field in the EXOTECH bands.

The measured atmospheric parameters had to be elaborated in a similar way. As these refer to an infinite atmosphere, values of the atmospheric parameters at flight altitude (1000 m) were obtained on the basis of both experimental data and model calculations (Turner and Spencer, 1972; Salby and McClatahey, 1975).

In Table 8 the measured values of path radiance and transmittance are presented together with the values derived for the flight altitude of 1000 m.

TABLE 8 PATH RADIANCE AND TRANSMITTANCE MEASURED ON THE GROUND (EXOTECH) AND CALCULATED FOR THE GROUND AND AN ALTITUDE OF 1000 m (DAEDALUS)

| Bands (nm) | | Transmittance | | | Path radiance (mW cm$^{-2}$ sr$^{-1}$ | |
|---|---|---|---|---|---|---|
| DAEDALUS | EXOTECH | measured ground | calculated ground | calculated 1000 m | ground | 1000 m |
| 500-550 | | | 0.65 | 0.85 | 0.141 | 0.0395 |
| | 498-596 | 0.68 | | | | |
| 500-600 | | | 0.70 | 0.89 | 0.103 | 0.0315 |
| 600-650 | | | | | 0.079 | 0.0265 |
| | 580-706 | 0.75 | | | | |
| 650-690 | | | 0.76 | 0.88 | 0.049 | 0.0175 |
| | 697-819 | 0.81 | | | | |
| 700-790 | | | 0.80 | 0.89 | 0.078 | 0.031 |
| 800-890 | | | 0.79 | 0.87 | 0.048 | 0.022 |
| | 767-974 | 0.80 | | | | |
| 920-110 | | | 0.78 | 0.83 | 0.45 | 0.025 |

The errors in the ground measurement of the spectral reflectance factors are mainly due to the following factors:

a) the absolute calibration of the field radiometer,

b) the variability of ground surfaces and the Lambertan assumption made for these surfaces,

c) the atmospheric instability and time elapsed between measurements of incoming irradiance and of reflected radiance.

An analysis of these errors was carried out and their combined effect has been evaluated.

The same analysis was performed for the spectral reflectance factors derived from the multi-spectral scanner data which is calibrated in terms of power which reaches the scanner.

In this case the spectral reflectance factor at ground level is given by the equation:

$$R_i = \pi \frac{\frac{P_i}{A_R \Omega_R} - Lp_i}{\tau_i I_i}$$

where:

$P_i$ = power received by the multi-spectral scanner in band i and recorded on CCT (W)

$I_i$ = global hemispherical incoming irradiance measured on the ground ($Wcm^{-2}$)

$\tau_i$ = transmittance at 1000 m height

$Lp_i$ = path radiance at 1000 m height ($Wcm^{-2}sr^{-1}$)

$A_R$ = area of the ground seen through the IFOV of the scanner from 1000 m height ($cm^{-2}$)

$R$ = effective optical aperture of the scanner ($a_o h^{-2}$)

Due to lack of information no error in the calibration of the multi-spectral scanner had to be assumed, though this assumption is certainly not true. The only errors which have been considered are due to:

- instability of the atmosphere
- errors in the measurement of $\tau$, $L_p$ and their evaluation at the flight altitude of 1000 m
- Lambertan assumption for ground surfaces

In Figs. 17-19 the spectral reflectance factor as a function of wavelength is presented for three surfaces, both as measured on the ground and as derived from airborne multi-spectral scanner measurements.

The types of surfaces are grassland (Fig. 17), ploughed bare soil (Fig. 18) and burnt stubble (Fig. 19). Data for stubble are not reported due to the low reliability of a single measurement made on this surface.

The errors evaluated for both the ground and airborne data are indicated only for the EXOTECH (LANDSAT) bands where a comparison between the two methods was possible.

## 3.2 Conclusions

It appears from Figs. 17-19 that the agreement between ground measured and airborne reflectance factors is satisfactory mainly for the lower wavelength bands. Here the agreement is more or less in the limit of the errors evaluated. At the higher wavelength bands, and especially on grassland, there is an increasing discrepancy between the two measurements. Better results might have been obtained by using the same bands for the field radiometer and the airborne scanner or by employing a continuous spectro-radiometer in the field to integrate data over the MSS bands. Even then, the absolute calibration of instruments for this type of measurements poses a major problem. It seems that the systematic discrepancy in



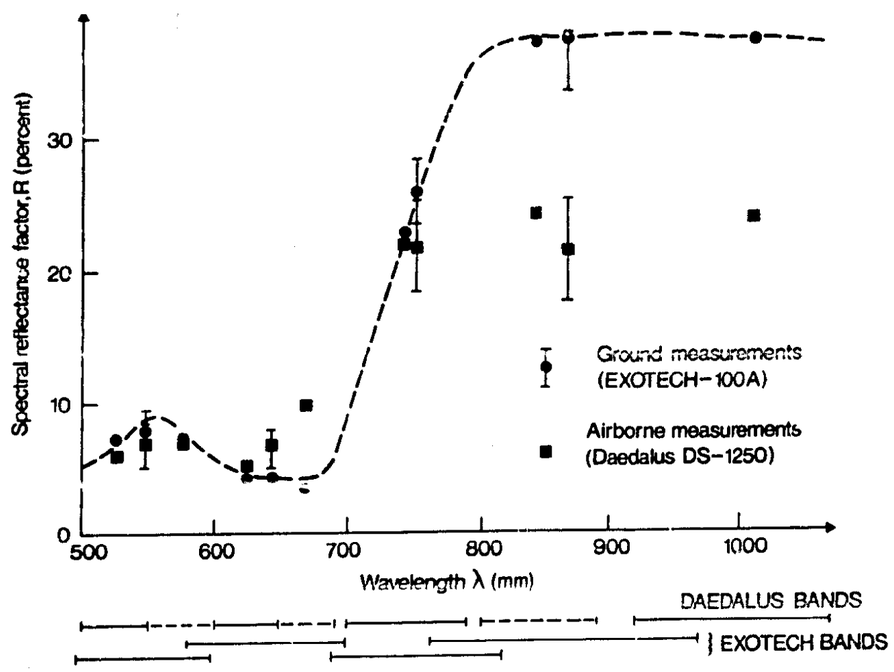


FIGURE 17 Spectral reflectance factor, R, of grassland measured at various wavelengths on the ground and by airborne MSS

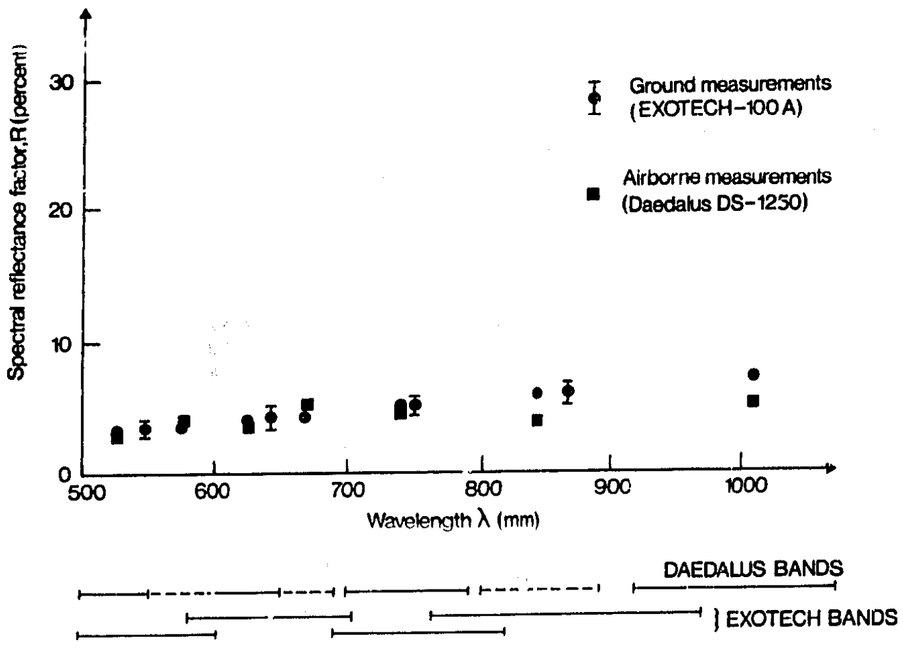


FIGURE 18 Spectral reflectance factor, R, of bare earth measured for various wavelengths on the ground and by airborne MSS

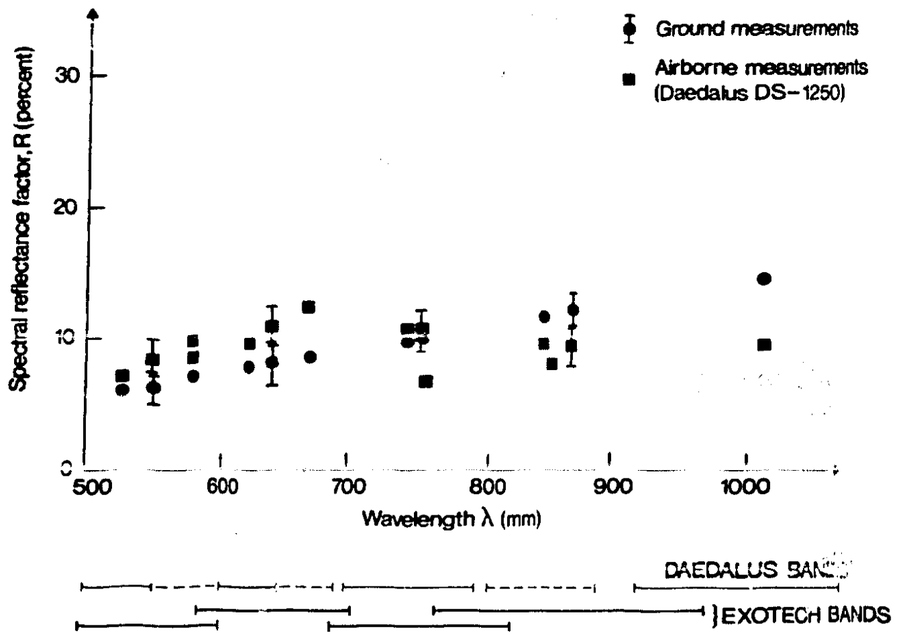


FIGURE 19 Spectral reflectance factor, R, of burnt stubble measured for various wavelengths on the ground and by airborne MSS

the near infra-red channels may be attributed both to the fact that bands are not easily and directly comparable and to a systematic error in the MSS calibration which gives constantly a lower value for the recorded power.

In fact, the values of the near infra-red spectral reflectance factor for grassland measured on the ground agree better with data from the literature than the values obtained from the airborne multi-spectral scanner. This strengthens the hypothesis of a systematic error in the calibration of the airborne multi-spectral scanner.

### 3.3 Correction of the Scan Angle Effect on the Spectrometric Values

As the scan angle of the Daedalus instrument used for the flight is 77°, the variation of the atmospheric thickness along the scan line causes a variation in the atmospheric effect from the centre of the line towards the edges, with a resulting systematic effect in the data acquired which must be corrected. Due to the difficulty in implementing a deterministic correction scheme which requires an accurate knowledge of the physical phenomena as a function of angle, the statistical approach known as along track averaging was preferred and applied to thermal and visible data.

Along the strip of acquired data, the mean values of the one pixel columns of data are calculated from edge to edge of the strip. A polynomial fitting of the mean values along the scan line is then used to describe the general trend of the effect. If the effect is absent or negligible, the fitted curve results in a straight horizontal line. The difference between the fitted curve and the value at the central column element (nadir point) calculated at each column position gives the correction to be applied to the value of the element in this position, in every scan line. The data also showed a loss of contrast towards the edges, and so it



was decided to also correct the variance in a similar fashion.

The correction curves exhibit a noticeable, although asymmetrical, variation for both the mean and variance for the day thermal and visible data and on the mean for night thermal data, while the effect on the variance is almost negligible for the night thermal data.

The data were then corrected for atmospheric absorption and scattering using the results already described.

## 4 APPLICATIONS OF DIGITAL MODELS

Application of digital models to estimate the evaporation and soil moisture status of the experimental sites has progressed through several stages. Initially, the Tellus (Rosema *et al.*, 1978) and Tergra (Soer, 1980) models were applied to sets of data produced from the overflights to gain experience with running the models. Some sensitivity testing of the models was then performed to find the range of variations of the input variables which are allowable without affecting the output of the models. The models were then run using data from individual fields, and work is now progressing in simplifying the models for operational use, as at present they are very fully and explicitly parameterized, and on producing maps of evaporation and soil moisture status. As this work is continuing, the details will be reported later, and only an outline presented here.

### 4.1 Tergra Model Sensitivity Studies

The Tergra model (Soer, 1980) was developed to predict regional evapotranspiration and soil moisture conditions from remotely sensed surface temperatures. Incoming radiation values, windspeed, air temperature, air humidity and parameters that are related to the vegetative cover and the soil are required as input.

The Tergra model is a steady state resistance model: the transport of water from the soil into the atmosphere is assumed to be governed by four resistances in series. These are the soil moisture $R_{soil}$ and plant resistance $R_{plant}$ for moisture flow and the stomatal resistance $R_{stomatal}$ and aerodynamic resistance $R_{atmosphere}$ for vapour flow.

The model sensitivity is difficult to predict because of the feedback mechanisms involved. The sensitivity of the model to its inputs was tested using simulation, both so that the model may be simplified for operational use and to check the internal consistency of the model.

The simulation period was from 5 a.m. till midnight G.M.T. Smoothed curves of the meteorological input parameters such as short wave incoming radiation, air temperature and water vapour pressure were used in the calculations while long-wave incoming radiation was calculated with a Brunt type equation. The vegetation was assumed to be a 7 cm high grass cover on a loam soil. The pF-curve and hydraulic conductivity-soil moisture content relationship were taken from the literature. Changes in capillary rise were not considered. The input used in the model is shown in Figure 12, and the changes in soil parameters given in Table 9.

TABLE 9 EFFECT OF UNCERTAINTY OF PARAMETERS ON CALCULATED ET VALUES UNDER WET AND DRY SOIL CONDITIONS

| | Parameter | | | | WET SOIL PSIS=-10kPa | | DRY SOIL PSIS=-500kPa | | MEDIUM DRY SOIL PSIS=-100kPa | |
|---|---|---|---|---|---|---|---|---|---|---|
| Meaning of Parameter | Name | Ref. value | Changed value | Change % | ET (mm) | dET/dpar | ET (mm) | dET/dpar | ET (mm) | dET/dpar |
| Initial soil moisture pot. (kPa) | PSIS | | | | | | | | | |
| Pore volume | THETAS | 0.51 | 0.54 | 6 | 2.37 | - | 1.13 | - | | |
| Exponent PSI-THETA relation | BL | 0.29 | 0.32 | 10 | 2.37 | - | 0.92 | 1.9 | 2.30 | - |
| Rest value saturation (VP) | SR | 0.03 | 0.04 | 33 | 2.37 | - | 1.13 | - | | |
| Soil density ($g/cm^3$) | D | 1.65 | 1.82 | 10 | 2.37 | - | 1.13 | - | | |
| Soil organic matter (WP) | SO | 1 | 2 | 100 | 2.37 | - | 1.13 | - | | |
| Saturated conductivity (m/day) | AKS | 0.06 | 0.072 | 20 | 2.37 | - | 1.22 | 0.4 | 2.31 | 0.02 |
| Air entry value (kPa) | PSIA | -5 | -6 | 20 | 2.37 | - | 1.37 | 1.1 | 2.31 | 0.02 |
| Saturated heat cond. (N/m/K) | HCS | 1.40 | 1.54 | 10 | 2.37 | - | 1.13 | - | | |
| Dry heat conductivity (N/m/K) | HCD | 0.20 | 0.22 | 10 | 2.37 | - | 1.13 | - | | |
| Global crop height (m) | GHC | 0.07 | 0.08 | 14 | 2.42 | 0.16 | 1.15 | 0.13 | | |
| Plant diff. resist. factor (day) | RPL | 12500 | 15000 | 20 | 2.27 | 0.22 | 1.10 | 0.13 | | |
| Root dens. resist. factor (mm) | RD | 3.7 | 4.5 | 20 | 2.37 | - | 1.03 | 0.44 | 2.30 | - |
| Effective rooting depth (m) | DD | 0.5 | 0.6 | 20 | 2.37 | - | 1.14 | 0.04 | 2.30 | - |
| Dummy reflection coefficient | REFL | 0.23 | 0.253 | 10 | 2.30 | 0.30 | 1.10 | 0.27 | | |
| Emission coefficient | EC | 0.95 | 0.99 | 5 | 2.32 | 0.42 | 1.10 | 0.54 | | |

TABLE 10 EFFECT OF CHANGES IN RESISTANCE ON EVAPOTRANSPIRATION AT THREE DIFFERENT WINDSPEEDS

| | | Windspeed (u) | | | | | | | | |
|---|---|---|---|---|---|---|---|---|---|---|
| | | u = 1 m/s | | u = 3 m/s | | | | | u = 7 m/s | |
| | Resistance | ET (mm) | ΔET (%) | ET (mm) | ΔET (%) | R at 1 p.m s,(s/m) | Change in temp. gradient above the crop at 1 p.m | Change in vapour press. gradient above the crop at 1 p.m | ET (mm) | ΔET (%) |
| | R unchanged | 2.26 | | 2.37 | | | | | 2.89 | |
| WET | Rplant = Rplant * 1.5 | 2.11 | - 6.6 | 2.12 | -10.6 | $1.08 \times 10^9$ | not calcul. | not calcul. | 2.42 | -15. |
| SOIL | Rsoil = Rsoil * 1.5 | 2.26 | - | 2.37 | - | 41840 | idem | idem | 2.89 | - |
| | Ratm. = Ratm. * 1.5 | 2.17 | - 4.0 | 2.20 | - 7.2 | 47.0 | idem | idem | 2.63 | - 9. |
| | Rstom. = Rstom. * 1.5 | 2.17 | - 4.0 | 2.22 | - 6.3 | 32.4 | idem | idem | 2.60 | -10. |
| | R unchanged | 1.36 | | 1.13 | | | | | 1.12 | |
| DRY | Rplant = Rplant * 1.5 | 1.29 | - 5.1 | 1.05 | - 7.1 | $1.08 \times 10^9$ | +3.3% | +1.7% | 1.04 | - 7 |
| SOIL | Rsoil = Rsoil * 1.5 | 1.18 | -13.2 | 0.93 | -17.7 | $3.3 \times 10^9$ | +8.2% | +4.3% | 0.91 | -18 |
| | Ratm. = Ratm. * 1.5 | 1.40 | + 2.9 | 1.18 | + 4.4 | 41.9 | +31.2% | +22.0% | 1.12 | - |
| | Rstom. = Rstom. X 1.5 | 1.22 | -10.3 | 0.97 | -14.2 | 194.9 | +5.5% | +3.9% | 0.94 | -16 |

As a first step the method employed by Nieuwenhuis and Klaassen (1978) was followed and the four resistances were successively increased by 50% for wet and dry soil conditions. Wet soil conditions were defined as a water content corresponding to a soil moisture potential $\psi_s$ of -10 kPa, and dry soil conditions were defined as a water content corresponding to a soil moisture potential of -500 kPa. The simulation was repeated for three windspeeds, each assumed to have been constant during the simulation period. The results of this analysis are presented in Table 10.

It seemed physically realistic that a change in one resistance affected one or more of the other resistances. Especially it could be postulated that changes in the soil and plant resistance to moisture transport, $R_{soil}$ and $R_{plant}$, should have an effect on the stomatal resistance $R_{stomatal}$. Therefore, for the case of a mean windspeed of 3 m/sec this interdependence has been estimated (Table 11). Various other soil and plant parameters have been changed. For every parameter the uncertainty in its estimate or determination was considered (Table 9.) The spread of this influence over the various resistances was also calculated (Table 12) for those parameters that appeared to have a significant influence on the evapotranspiration value.

TABLE 11 EFFECT OF ONE RESISTANCE ON OTHER RESISTANCES

| | Resistance Changed | $R_{plant}$ | $R_{soil}$ | $R_{atm.}$ | $R_{stom.}$ |
|---|---|---|---|---|---|
| WET SOIL | $R_{pl}=R_{pl} * 1.5$ | - | -1.5% | - | +75% |
| | $R_{soil}=R_{soil} * 1.5$ | - | - | - | - |
| | $R_{atm.}=R_{atm.} * 1.5$ | - | -1.0% | - | - 4% |
| | $R_{stom.}=R_{stom.} * 1.5$ | - | - | -1.0% | - |
| DRY SOIL | $R_{pl}=R_{pl} * 1.5$ | - | - | - | +10% |
| | $R_{soil}=R_{soil} * 1.5$ | - | - | - | +25% |
| | $R_{atm.}=R_{atm.} * 1.5$ | - | - | - | + 9% |
| | $R_{stom.}=R_{stom.} * 1.5$ | - | -3% | - | - |

TABLE 12 EFFECT OF UNCERTAINTY IN SIGNIFICANT PARAMETERS ON VARIOUS RESISTANCES

| Parameter | | | | Change in Various Resist. | | | | Change in Evapotranspiration |
|---|---|---|---|---|---|---|---|---|
| Name | Reference value | Changed value | Change % | $R_{plant}$ | $R_{soil}$ | $R_{atm.}$ | $R_{stom.}$ | ΔET |
| BL | 0.29 | 0.32 | 10.3 | +50% | | | +30% | -18.6% |
| AKC | 0.06 | 0.072 | 20 | -16.9% | | | -10.2% | +8.0% |
| SCIA | -5 | -6 | 20 | -40% | | | -25% | +21.2% |
| GHC | 0.07 | 0.08 | 14.3 | | | -4.8% | -4.5% | +1.8% |
| RD | 3.7 | 4.5 | 21.6 | +20.6% | | | +12.4% | -8.8% |

Table 12: Effect of Incertainty in Significant Parameters on Various Resistances.

Results may be summarized as follows:

*Changes in resistance at three different windspeeds (Table 10).*

Wet soil conditions:

Evapotranspiration increases with increasing windspeed. A change in $R_{soil}$ has no influence on evapotranspiration as $R_{plant}$ is about twenty-five times larger than $R_{soil}$. Thus, the sum ($R_{plant} + R_{soil}$) which regulates the amount of evapotranspiration is virtually independent of $R_{soil}$. At a windspeed of 1 m/sec the influence of $R_{plant}$, $R_{atm}$, and $R_{stom}$ on evapotranspiration are of the same order of magnitude. The model becomes more sensitive with increasing windspeed because of a higher evaporative demand, and as the influence of $R_{plant}$, $R_{atm}$, and $R_{stom}$ on evapotranspiration increase.

Dry soil conditions:

Evapotranspiration decreases with increasing windspeed and at this condition a rise in $R_{atm}$ results in increased evapotranspiration. Both phenomena may have the same cause, which may be found by considering the formulation of sensible heat and of latent heat fluxes respectively:

$$H = \frac{\rho Cp}{R_{atm}} \cdot (T_{PA} - T_{PO})$$

H = sensible heat ($w/m^2$)

$\rho Cp$ = heat capacity of the air (J/kg/K)

$T_{PA}$ = air temperature at reference height (K)

$T_{PO}$ = crop temperature (K)

and:

$$LE = \frac{\rho Cp}{\gamma} \cdot \frac{E_{AT} - E_{OS}}{R_{atm} + R_{stom}}$$

LE = latent heat ($w/m^2$)

$\gamma$ = psychrometer constant (Pa/K)

$E_{AT} - E_{OS}$ = water vapour deficit between sub-stomatal cavities and the atmosphere at reference height (Pa).

For a windspeed of 3 m/sec the following results were obtained: $R_{stom}$ is about five times larger than $R_{atm}$ and therefore an increase of $R_{atm}$ of 50% has a negligible effect on the sum ($R_{atm} + R_{stom}$) in eq. (2). At the same time the temperature gradient ($T_{PA} - T_{PO}$) in eq. (1) is not increasing as rapidly as $R_{atm}$ (31% against 50%) but ($E_{AT} - E_{OS}$) in eq. (2) is increasing more rapidly than ($R_{atm} + R_{stom}$). Hence, for a 50% increase in $R_{atm}$ the sensible heat flux decreases and the latent heat flux increases, the combined effect being a higher evapotranspiration. The same reasoning explains the reduction in the latent heat flux with increasing wind speed. Increasing wind speed means a decrease of the aerodynamic resistance and under these circumstances the result is a decrease of evapotranspiration.



*Effect of Changes of One Resistance on Other Resistances (Table 11).*

Wet soil conditions:

The effect of changes in plant resistance on stomatal resistance is predominant under these conditions. An increase of plant resistance by 50% results in an increase of the stomatal resistance by as much as 75%. An increase of $R_{stom}$ by 75% results in the same reduction of evapotranspiration as the resistance to plant moisture transport is defined dependent on the stomatal resistance. Changes in other resistances have very small or negligible effects.

Dry soil conditions:

Under dry soil conditions the soil moisture resistance is predominant. An increase of the soil moisture resistance by 50% results in an increase of $R_{stom}$ of only 25% whereas the reduction in evapotranspiration is larger than when $R_{stom}$ is increased independently by 50% (-17.7% against - 14.2%, table 10). This is caused by the fact that an independent increase of the stomatal resistance is not "accepted" by the model: during the successive iterations the value of the stomatal resistance is reduced again until the new value is only about 20% larger than the original one, at least during the hours in which the major part of the daily evapotranspiration takes place.

*Effect of Uncertainty of Parameters on Calculated ET Values Under Wet and Dry Soil Conditions (Table 9)*

Wet soil conditions:

Changes in the soil parameters considered had no effect on the evapotranspiration flux. Under these conditions the state of potential evapotranspiration is reached and then apparently the system is very stable. Only the plant moisture resistance is a factor that must be taken into account, as was already known from Table 10. The potential evapotranspiration flux can only be changed by differences in crop length and radiation values, as clearly illustrated by the effects of changes in global crop height, reflectivity and emissivity.

Dry soil conditions:

Some soil parameters play a role in determining the evapotranspiration flux. Among these the importance of air entry value $\psi_A$ must be noted, although this parameter is difficult to determine precisely. Also the errors in the exponent of the soil tension-soil water content relationship and in the hydraulic conductivity can change the amount of evapotranspiration flux significantly. Fortunately, these two parameters may be determined more precisely than the air entry value. Another factor that becomes important under dry conditions is the root density resistance factor, RD, also difficult to determine. Thus, the factors that determine the thermal properties of the soil do not greatly affect evapotranspiration, as the soil heat flux plays a minor role in the energy balance equation when the soil is completely covered by vegetation. Therefore, the determination of the soil density, percentage organic matter and saturated and dry heat capacities does not need to be very precise. For the saturated and dry heat capacity a calculation using the method of De Vries or even an estimation with the help of relationships given by De Vries seems sufficient. The global crop height, plant diffusion resistance, reflectivity and emissivity have the same proportional effect as under wet conditions and consequently they must be determined with the same precision for the whole soil moisture range.

In this analysis a dry soil was defined as having a soil moisture tension of 500 kPa (5000 mbar or pF = 3.7). This is in fact a very extreme situation, especially for the usually rather humid conditions of Western Europe. Therefore, for those factors that have a strikingly different influence on evapotranspiration depending on the soil moisture situation, a more realistic value was taken of a soil moisture tension of 100 kPa for dry conditions. From the results presented in the last column of Table 9 one can conclude that under this condition the importance of errors in the exponent of the soil tension/soil moisture content relationship, the saturated conductivity, the air entry value, the root density and rooting depths are much reduced. Therefore, in the more usual range between pF = 2 and pF = 3 the soil moisture parameters are not critical. A soil having a pF curve with a better defined break point might give different results and the sensitivity analysis should be repeated for such a case.

*Effect of Uncertainty of Parameters on Resistances (Table 12)*

The results are consistent with the previous discussion, and the most striking feature is again the quite constant relation between soil and stomatal resistances. The effect of an increased crop height on both aerodynamic and stomatal resistances stems from the iteration procedure of the Tergra model with regard to a zero energy balance at the soil surface.

*Conclusions of the Sensitivity Analysis*

In the soil moisture tension range between pF 2 and pF 3 which is usual in the humid climate of Western Europe, evapotranspiration is only slightly affected by soil parameters. In this range of potential evapotranspiration the rate of water loss is almost exclusively determined by the atmospheric evaporative demand. These confirm previous work. It would be worthwhile to repeat the sensitivity analysis for semi-arid conditions and for other soil types to see what differences there are. Results would be the same as found here under all conditions where plants are transpiring potentially.

## 4.2 Testing the Tellus Model

The model was tested; during this test a number of problems concerning the model arose. The first problem concerned the numerical value of the soil heat capacity used in the model. The value of $2 \times 10^7$ J/m$^3$/K originally employed exceeds by about a factor of ten the values actually measured. These range approximately from $1 \times 10^6$ J/m$^3$/K for a dry soil to $3 \times 10^6$ J/m$^3$/K for a wet soil. This high value is used to speed up the program by permitting the large time step of one hour, to minimize the total computation calculation time. Errors introduced by this method should be small. The validity of this assumption for the Grendon data was investigated.

The second problem concerned the assumption of a constant surface relative humidity. In the original form of the model this assumption led to excessive condensation. The model was modified to ignore condensation, but positive values of the latent heat flux were nevertheless entered into the energy balance equation and so into the determination of simulated surface temperatures.

The results of the model are presented in the form of standard look-up tables indicating day and night surface temperature and daily cumulative evaporation for various combinations of thermal inertia and surface relative humidity for the bare soil site.

The program was first run with a value of the soil heat capacity of $2 \times 10^6$ J/m$^3$/K,



a mean value for the soil of the Grendon area. This value of the heat capacity had to be combined with a small time step of 36 seconds in order not to change the Fourier coefficient used in the Du Fort-Frankel scheme that simulates the temperature profile below the soil surface.

The results of this run are shown in Table 13 and they are assumed to be "correct" as the soil heat capacity was an experimentally measured value.

TABLE 13 TELL-US LOOK-UP TABLE FOR A REALISTIC HEAT CAPACITY VALUE OF $2 \times 10^6$ J/m$^3$/K. CALCULATION TIME STEP: 36 sec
(Negative values of evaporation are condensation)

| Thermal Inertia | | Surface Relative Humidity 0.0 | 0.20 | 0.40 | 0.60 | 0.80 | 1.00 |
|---|---|---|---|---|---|---|---|
| 800. | D.temp. | 44.2 | 34.8 | 29.9 | 26.6 | 24.2 | 22.3 |
| | N.temp. | 7.1 | 4.8 | 3.2 | 0.0 | -0.8 | -1.4 |
| | C.evap. | -5.6 | -2.1 | -0.1 | 1.3 | 2.2 | 2.8 |
| 1200. | D.temp. | 41.7 | 33.5 | 29.0 | 25.9 | 23.6 | 21.8 |
| | N.temp. | 9.4 | 6.9 | 5.2 | 3.9 | 2.6 | 1.6 |
| | C.evap. | -5.6 | -2.2 | -0.3 | 1.0 | 2.0 | 2.7 |
| 1600. | D.temp. | 39.5 | 32.2 | 28.1 | 25.2 | 23.0 | 21.2 |
| | N.temp. | 11.0 | 8.4 | 6.6 | 5.3 | 4.2 | 3.2 |
| | C.evap. | -5.6 | -2.3 | -0.4 | 0.9 | 1.9 | 2.6 |
| 2000. | D.temp. | 37.6 | 31.1 | 27.3 | 24.5 | 22.4 | 20.8 |
| | N.temp. | 12.2 | 9.5 | 7.7 | 6.3 | 5.2 | 4.3 |
| | C.evap. | -5.5 | -2.4 | -0.5 | 0.8 | 1.8 | 2.6 |

A second simulation run was carried out using the excessively high value of the soil heat capacity of $2 \times 10^7$ J/m$^3$/K combined with a time step of 1 hour. This combination was originally used in the program. The difference between these results and the "correct" surface temperatures and evaporation are shown in Table 14. The figures show that day surface temperatures differ by less than one degree and usually by less than 0.5°C. In addition the differences of the cumulative evaporation are very small: 0.3 mm or less. Night surface temperatures proved to be sensitive to the heat capacity value employed: temperatures simulated with the high soil heat capacity were considerably lower than the "correct" values, the difference ranging from -1.3°C for a saturated soil to -2.7°C for dry soil.

The thermal inertia range from 800 to 2000 J/m$^2$/s$^{1/2}$/k roughly corresponds to the maximum moisture content range from dry to saturated for Oxford clay, the soil type of the test site. The look-up table in Table 13 shows that for a given surface relative humidity the differences in night-time temperatures range between five and six degrees. This means for example that an error of two degrees in the simulated night temperature may result in an underestimation of the thermal inertia by 400 units. Translated into soil moisture this would represent an error of approximately 15 percent by volume of moisture or one third of the total soil moisture range, which seems quite unacceptable for practical purposes.

TABLE 14 THE DIFFERENCE BETWEEN A TELL-US LOOK-UP TABLE CACLUATED WITH A HIGH HEAT CAPACITY OF 2 x $10^7$ J/$m^3$/K, TIME STEP 3600 sec (Negative values of evaporation are condensation)

| Thermal Inertia | | Surface Relative Humidity | | | | | |
|---|---|---|---|---|---|---|---|
| | | 0.0 | 0.20 | 0.40 | 0.60 | 0.80 | 1.00 |
| 800. | D.temp. | +0.7 | +0.3 | +0.3 | +0.3 | +0.3 | +0.3 |
| | N.temp. | -2.7 | -2.3 | -2.1 | -0.7 | -0.8 | -2.2 |
| | C.evap. | +0.0 | -0.1 | -0.1 | -0.1 | 0.0 | +0.0 |
| 1200. | D.temp. | +0.4 | +0.2 | +0.2 | +0.2 | +0.2 | +0.3 |
| | N.temp. | -2.2 | -1.9 | -1.8 | -1.7 | -1.5 | -1.4 |
| | C.evap. | +0.0 | 0.0 | 0.0 | 0.0 | -0.1 | -0.1 |
| 1600. | D.temp. | 0.0 | -0.1 | -0.1 | 0.0 | +0.1 | +0.1 |
| | N.temp. | -1.9 | -1.6 | -1.5 | -1.4 | -1.4 | -1.4 |
| | C.evap. | +0.0 | +0.1 | +0.1 | -0.1 | -0.2 | -0.3 |
| 2000. | D.temp. | -0.6 | -0.4 | -0.3 | -0.2 | -0.1 | 0.0 |
| | N.temp. | | | -1.3 | -1.2 | -1.2 | -1.3 |
| | C.evap. | | | +0.2 | -0.2 | -0.3 | -0.3 |

One may accordingly conclude that the high soil heat capacity employed to speed up the calculations may not be used in the present case. However, neither is the use of the alternative realistic heat capacity value very attractive because of the accompanying small calculation time step. The computation time for the table shown in Table 13 is a full five minutes, against eleven seconds needed to produce the results seen in Table 14. Therefore, when a mass production of look-up tables is required, it seems best to use the fast version and to estimate the night temperature correction with the help of a small number of look-up tables derived with the slow version for some well chosen combinations of parameters.

A simple finite difference scheme was tried, instead of the Du Fort-Frankel scheme for the calculation of the soil heat flux. In Table 15 a look-up table calculated with the simpler algorithm is shown. It should be comparable with Table 13 and the difference between the two tables is presented in Table 16. Maximum differences in day surface temperature are 1-2°C, in night surface temperature 0.6°C, but on average differences are much smaller and the resemblance between the two tables is rather close. An exception has to be made for conditions of heavy condensation (at the left-hand side of the look-up table, where differences of cumulative evaporation amount to 1-5 mm). Here, the calculation time is reduced by a factor of five relative to the "correct" method in Table 13.

The program was re-written so that the relationship between soil moisture content and thermal inertia may be changed easily. Heat capacity and thermal conductivity may then be written as a function of volumetric moisture content and from these values the corresponding thermal inertia value is calculated. In order to study the effect of a constant heat capacity through the moisture content range compared to a more precise value varying with soil moisture, Tables 17 and 18 were produced.



TABLE 15 LOOK-UP TABLE CALCULATED WITH A SIMPLIFIED FORMULATION OF THE GROUND HEAT FLUX. Heat capacity: 2 x $10^6$ J/$m^3$/K. Calculation time step: 300 sec Depth step: 2.5 cm (Negative values for C. evap. mean condensation)

| Thermal Inertia | | Surface Relative Humidity | | | | | |
|---|---|---|---|---|---|---|---|
| | | 0.0 | 0.20 | 0.40 | 0.60 | 0.80 | 1.00 |
| 800. | D.temp. | 44.1 | 34.3 | 29.4 | 26.2 | 23.9 | 22.0 |
| | N.temp. | 7.5 | 5.2 | 3.4 | 0.6 | -0.3 | -0.8 |
| | C.evap. | -7.0 | -2.6 | -0.3 | 1.3 | 2.3 | 3.0 |
| 1200. | D.temp. | 42.2 | 33.3 | 28.7 | 25.7 | 23.4 | 21.6 |
| | N.temp. | 9.6 | 7.0 | 5.3 | 3.9 | 2.7 | 1.8 |
| | C.evap. | -7.0 | -2.8 | -0.5 | 1.1 | 2.2 | 2.9 |
| 1600. | D.temp. | 40.4 | 32.4 | 28.1 | 25.2 | 23.0 | 21.3 |
| | N.temp. | 11.0 | 8.3 | 6.5 | 5.1 | 4.0 | 3.1 |
| | C.evap. | -7.0 | -2.9 | -0.6 | 1.0 | 2.1 | 2.9 |
| 2000. | D.temp. | 38.8 | 31.3 | 27.5 | 24.7 | 22.6 | 21.0 |
| | N.temp. | 11.8 | 9.1 | 7.3 | 6.0 | 4.9 | 4.0 |
| | C.evap. | -7.0 | -3.0 | -0.7 | 0.9 | 2.0 | 2.9 |

TABLE 16 DIFFERENCE BETWEEN LOOK-UP TABLES 15 AND 13

| Thermal Inertia | | Surface Relative Humidity | | | | | |
|---|---|---|---|---|---|---|---|
| | | 0.0 | 0.20 | 0.40 | 0.60 | 0.80 | 1.00 |
| 800. | D.temp. | -0.2 | -0.5 | -0.5 | -0.4 | -0.3 | -0.2 |
| | N.temp. | +0.5 | +0.3 | +0.2 | +0.6 | +0.6 | +0.5 |
| | C.evap. | +1.5 | +0.6 | +0.2 | 0.0 | +0.1 | +0.2 |
| 1200. | D.temp. | +0.5 | -0.2 | -0.2 | -0.2 | -0.2 | -0.1 |
| | N.temp. | +0.2 | +0.1 | 0.0 | 0.0 | +0.1 | +0.2 |
| | C.evap. | +1.5 | +0.6 | +0.2 | 0.0 | +0.2 | +0.2 |
| 1600. | D.temp. | +0.9 | +0.2 | 0.0 | 0.0 | 0.0 | 0.0 |
| | N.temp. | 0.0 | 0.0 | -0.2 | -0.2 | -0.2 | -0.1 |
| | C.evap. | +1.5 | +0.6 | +0.2 | +0.1 | +0.2 | +0.2 |
| 2000. | D.temp. | +1.2 | +0.4 | +0.2 | +0.2 | +0.2 | +0.2 |
| | N.temp. | -0.4 | -0.4 | -0.4 | -0.3 | -0.3 | -0.3 |
| | C.evap. | +1.5 | +0.6 | +0.2 | +0.1 | +0.2 | +0.3 |

TABLE 17 **LOOK-UP TABLE CALCULATED WITH HEAT CAPACITY AND THERMAL CONDUCTIVITY AS A FUNCTION OF THE VOLUMETRIC MOISTURE CONTENT (THETA). The ground heat flux is calculated in a simplified way.**

| Thermal Inertia (THETA) | | Surface Relative Humidity | | | | | |
|---|---|---|---|---|---|---|---|
| | | 0.0 | 0.20 | 0.40 | 0.60 | 0.80 | 1.00 |
| | D.temp. | 32.2 | 32.2 | 28.8 | 25.8 | 23.6 | 21.8 |
| 1020. | N.temp. | 1.7 | 1.7 | 1.6 | 1.3 | 1.1 | 0.8 |
| (0.050) | C.evap. | 0.0 | 0.0 | 0.7 | 1.6 | 2.4 | 3.0 |
| | D.temp. | 30.9 | 30.9 | 28.2 | 25.3 | 23.2 | 21.5 |
| 1383. | N.temp. | 3.3 | 3.3 | 3.2 | 3.0 | 2.8 | 2.4 |
| (0.200) | C.evap. | 0.0 | 0.0 | 0.6 | 1.5 | 2.2 | 2.9 |
| | D.temp. | 30.1 | 30.1 | 27.8 | 25.0 | 22.9 | 21.2 |
| 1619. | N.temp. | 4.0 | 4.0 | 4.0 | 3.8 | 3.5 | 3.0 |
| (0.300) | C.evap. | 0.0 | 0.0 | 0.5 | 1.4 | 2.2 | 2.8 |
| | D.temp. | 29.1 | 29.1 | 27.2 | 24.6 | 22.6 | 21.0 |
| 1968. | N.temp. | 4.9 | 4.9 | 4.9 | 4.6 | 4.4 | 3.8 |
| (0.450) | C.evap. | 0.0 | 0.0 | 0.4 | 1.3 | 2.1 | 2.8 |

TABLE 18 **LOOK-UP TABLE CALCULATED ACCORDING TO THE SAME SCHEME BUT WITH A FIXED HEAT CAPACITY (2 x $10^6$ J/$m^3$/K)**

| Thermal Inertia | | Surface Relative Humidity | | | | | |
|---|---|---|---|---|---|---|---|
| | | 0.0 | 0.20 | 0.40 | 0.60 | 0.80 | 1.00 |
| | D.temp. | 32.2 | 32.2 | 28.8 | 25.8 | 23.5 | 21.8 |
| 1020. | N.temp. | 1.0 | 1.0 | 1.0 | 0.7 | 0.5 | 0.2 |
| | C.evap. | 0.0 | 0.0 | 0.7 | 1.6 | 2.3 | 2.9 |
| | D.temp. | 30.9 | 30.9 | 28.1 | 25.3 | 23.1 | 21.4 |
| 1383. | N.temp. | 3.1 | 3.1 | 3.1 | 2.8 | 2.6 | 2.3 |
| | C.evap. | 0.0 | 0.0 | 0.6 | 1.5 | 2.2 | 2.9 |
| | D.temp. | 30.1 | 30.1 | 27.7 | 25.0 | 22.9 | 21.2 |
| 1619. | N.temp. | 4.0 | 4.0 | 3.9 | 3.7 | 3.5 | 3.0 |
| | C.evap. | 0.0 | 0.0 | 0.5 | 1.4 | 2.2 | 2.8 |
| | D.temp. | 29.1 | 29.1 | 27.2 | 24.6 | 22.6 | 21.0 |
| 1968. | N.temp. | 5.0 | 5.0 | 5.0 | 4.8 | 4.5 | 3.9 |
| | C.evap. | 0.0 | 0.0 | 0.4 | 1.3 | 2.1 | 2.8 |



One may notice that when a fixed heat capacity is used (Table 14) the night temperatures are underestimated in the dry moisture content range and overestimated in the wet range compared to allowing it to vary. However, the differences are so small (0.7°C maximum) that simulation with a constant heat capacity value of 2 x $10^6$ J/$m^3$/K is justified.

One of the simplifications in the Tellus model was the assumption of a constant surface relative humidity. For the lower values of surface relative humidity, and given the rather moist atmosphere in Grendon, the program calculates net amounts of condensation over a period of one day. Condensation is accompanied by the release of latent heat of condensation so when heavy condensation occurs the simulated surface temperatures go to very high values (Tables 13 and 14). In the modified model, condensation is not included in the summation calculating the cumlative evaporation, but its effect on the surface temperature remains. It is clear that from the physical point of view this solution must be considered as most unfortunate.

In search of an alternative solution a reduction in condensation was tried by introducing a variable surface relative humidity value. This resets it to its original value at every calculation time step. In cases when the latent heat flux becomes positive, surface relative humidity is increased automatically until the latent heat flux becomes zero. If the maximum relative humidity of 1.0 has been reached and the latent heat flux is still positive, this value is accepted and entered into the energy balance equation. Although from a purely mathematical point of view this solution may be questionable, it seems to correspond to the physical phenomenon that the surface relative humidity has to rise before condensation may occur. Almost the same results were achieved and a considerable amount of calculation time was saved by a simpler approach, that if the latent heat flux was positive, then a value of zero was entered into the energy balance equation.

The result of these calculations is given in Tables 19 and 20. As shown in Table 19, the temperature range of the look-up table becomes considerably more restricted compared to a look-up table without correction for excessive condensation, for instance the results in Table 15. The differences between the surface temperatures in Tables 19 and 15 are shown in Table 20. These differences are very high, more than 10°C for low surface relative humidities, at the left-hand side of the table, and somewhat smaller for high surface relative humidities, especially with regard to the day temperature estimates.

The restricted surface temperature range of the look-up table, Table 19, implies that fewer temperature combinations may be accommodated on one table. This should reduce the chance that by simulating with erroneous parameter values, the measured surface temperature combination can be found on the look-up table, though at the wrong surface relative humidity or thermal inertia values.

The measured airborne scanner day and night temperatures of the bare soil field at Grendon were analyzed with the help of a statistical computer program. The radiative temperatures were the following:

ght temperature (minimum) at 4.45 GMT: 4.3°C ± 0.3°C s.d.

day temperature (maximum) at 13.00 GMT: 26.8°C ± 0.8°C s.d.

Assuming an emissivity of 0.975 the night temperature was estimated as 6.1°C and the day temperature as 28.7°C. According to the look-up table of Figure 13 this night/day temperature pair corresponds to a thermal inertia of about 1400 and a surface relative humidity of 0.30, whereas net condensation is calculated for the whole day. As pointed out before, this look-up table does not underestimate the

TABLE 19 LOOK-UP TABLE CALCULATED WITH A SCHEME ENTERING A LATENT HEAT FLUX VALUE OF ZERO INTO THE ENERGY BALANCE EQUATION WHEN CONDENSATION OCCURS. This Table should be comparable with Table 15

| Thermal Inertia | | Surface Relative Humidity | | | | | |
|---|---|---|---|---|---|---|---|
| | | 0.0 | 0.20 | 0.40 | 0.60 | 0.80 | 1.00 |
| 800. | D.temp. | 33.1 | 33.1 | 29.2 | 26.1 | 23.8 | 22.0 |
| | N.temp. | -0.9 | -0.9 | -1.0 | -1.2 | -1.5 | -1.6 |
| | C.evap. | 0.0 | 0.0 | 0.7 | 1.7 | 2.4 | 3.0 |
| 1200. | D.temp. | 31.5 | 31.5 | 28.4 | 25.5 | 23.3 | 21.6 |
| | N.temp. | 2.2 | 2.2 | 2.1 | 1.8 | 1.6 | 1.3 |
| | C.evap. | 0.0 | 0.0 | 0.6 | 1.5 | 2.3 | 2.9 |
| 1600. | D.temp. | 30.1 | 30.1 | 27.8 | 25.0 | 22.9 | 21.3 |
| | N.temp. | 3.9 | 3.9 | 3.8 | 3.6 | 3.4 | 2.9 |
| | C.evap. | 0.0 | 0.0 | 0.5 | 1.4 | 2.2 | 2.8 |
| 2000. | D.temp. | 29.0 | 29.0 | 27.1 | 24.6 | 22.6 | 21.0 |
| | N.temp. | 5.1 | 5.1 | 5.0 | 4.8 | 4.6 | 3.9 |
| | C.evap. | 0.0 | 0.0 | 0.4 | 1.3 | 2.1 | 2.8 |

TABLE 20 DIFFERENCE BETWEEN THE SURFACE TEMPERATURES IN TABLES 19 AND 15, SHOWING THE EFFECT OF HEAT OF CONDENSATION

| Thermal Inertia | | Surface Relative Humidity | | | | | |
|---|---|---|---|---|---|---|---|
| | | 0.0 | 0.20 | 0.40 | 0.60 | 0.80 | 1.00 |
| 800. | D.temp. | -11.0 | -1.2 | -0.2 | -0.1 | -0.1 | -0.1 |
| | N.temp. | -8.5 | -6.1 | -4.4 | -1.9 | -1.2 | -0.6 |
| 1200. | D.temp. | -10.7 | -1.9 | -0.3 | -0.2 | -0.1 | -0.1 |
| | N.temp. | -7.4 | -4.8 | -3.2 | -2.0 | -1.1 | -0.5 |
| 1600. | D.temp. | -10.3 | -2.3 | -0.3 | -0.1 | -0.1 | 0.0 |
| | N.temp. | -7.1 | -4.4 | -2.6 | -1.5 | -0.6 | -0.2 |
| 2000. | D.temp. | -9.9 | -2.6 | -0.3 | -0.1 | 0.0 | 0.0 |
| | N.temp. | -6.8 | -4.1 | -2.3 | -1.2 | -0.3 | -0.1 |



night temperatures as does the look-up Table 14. With Table 14 one should have found a thermal inertia of 1000, a surface relative humidity of 0.30 and also net condensation. In both tables there is an effect of increasing the simulated surface temperatures by condensation. As discussed before, this version of the model has a tendency to exaggerate dew formation. Furthermore, the weather on the day treated was warm and dry. Therefore, it seemed preferable to use a look-up table corrected for excess condensation as shown in Table 19, but surprisingly enough the measured temperature combination cannot be placed in the table. At first it was thought that this was due to the absence of wind during the night. Experience with grass has shown that under such circumstances the simulated surface temperature falls below the measured one, probably because the equations describing turbulent heat exchange fail under conditions of low wind speed. The calculated atmospheric resistance becomes very high, while in reality there may be a much lower limiting value. However, introducing a smaller atmospheric resistance brings no improvement in this case since it will be effective only if the surface temperature is lower than the air temperature.

In the absence of wind, local differences of air temperatures will arise because of the interaction between the surface and the air over it. Indeed, the measured air temperatures above the bare soil field at 4.50 GMT show a difference of almost 4°C with the air temperature recorded at the meteorological station. After insertion of these higher air temperatures during the hours of zero wind speed into the simulation data, the look-up table 5 was produced. In this table the measured surface temperature pair fits a thermal inertia of 1800 accompanied by a relative humidity of 0.30. This thermal inertia of 1800 corresponds to a volumetric moisture content of 0.37 (Table 17) Core samples of the upper 15 cm indicated a gravimetric moisture content of 0.[illegible] which should be in rather good agreement with the calculated value, assuming a soil apparent specific density of 1.1 to 1.2.

Rather little importance should be attributed to the agreement obtained between calculated and measured soil moisture because of all the corrections. It should only help to illustrate the ambiguity of the use of simulation models and the look-up tables they produce, without a proper examination of the assumptions inherent to the model. In the present case use of look-up Table 12 would have resulted in an estimated volumetric soil moisture content of 0.21, which is rather far from measured values.

Furthermore, due to the variability in air temperature to be expected over various surfaces at low or zero wind speed, the model must only be applied with circumspection.

## 4.3 Creation of Look-up Tables for Point-by-Point Plotting

To apply the Tellus model, an algorithm was developed (Rosema *et al.*, 1978) which calculates, for a given set of input parameters, a graph in the night temperature and day temperature coordinates made up of equi-thermal inertia and equi-relative surface humidity curves crossing each other. Each part of measured day and night temperatures results in a point contained within one of the irregular quadrilaterals of this lattice; the corresponding thermal inertia (THI) and relative surface humidity (RSH) values can then be determined by constructing the interpolated equi-THI and equi-RSH passing through the point. A second graph of equi-THI curves, in RSH and cumulative daily evaporation (CDE) coordinates, allows the calculation of CDE by starting from the already known RSH and the proper interpolated equi-THI corresponding to the THI value calculated in the first graph.

A set of routines has been written which perform the following sequence of actions

for each (Td, Tn) pair of thermal scanner data:

- localize the quadrilateral containing the point in Td, Tn coordinates;
- construct the interpolated equi-THI and equi-PSH passing through the point;
- determine THI and RSH values by linear interpolation between neighbouring values;
- construct the useful segment of the interpolated curve in the second graph by linear interpolation between the upper and lower bounding equi-THI;
- determine the CDE value by linear interpolation within this segment.

The above procedure leads to search and interpolation routines within a complex table with two entries (ESH and THI) and three values (Td, Tn, CDE) at each entry crossing.

If the surface temperatures are to be used pixel by pixel, the same must be done for albedo which is of great importance in the surface energy balance and which also varies pixel by pixel within a single field. The area is flat and so topography was ignored. Surface aerodynamic roughness is another important parameter and so the fields considered have been grouped into three broad classes: ploughed bare soil with roughness estimated to 0.015 m; stubble with roughness estimated to 0.020 m, and burnt stubble with roughness estimated to 0.010 m. Emissivity should be measured for each field surface type. Such measurements, however, are not available for the flight over Grendon. It was estimated that the range of variation should be from 0.96 to 0.97 for the fields considered, and as the model is hardly sensitive to this emissivity variation, a mean value of 0.965 was assumed for the whole area. As a result of this analysis, the procedure described had to be altered in the following way in order to:

- calculate with the Tellus model a series of look-up tables by allowing albedo to vary as input within a range;
- calculate this series of tables for a range of roughness values.

The following sequence of actions is then performed for each (Td, Tn, A) pixel of scanner data, A being albedo value:

- retrieve the field in which the given pixel is located and the roughness value attributed to this field.
- retrieve from the model look-up tables the two tables with albedo input values straddling the A value;
- calculate THI and RSH from (Td, Tn) in each table;
- determine the final THI and RSH values by linear interpolation between the two values calculated in the two tables,
- determine CDE.

The retrieval of the corresponding field identity and roughness value implies that a file has been constructed in which all the pixels in each of the fields considered (and not in the other fields) are replaced by index values equal to the proper field number (field identity) and that a correspondence between field number and roughness value is available. The various search and interpolating processes will thus work within and between tables generated by the Tellus algorithm, on a pixel by pixel basis with four variables: day temperature, night temperature, albedo and field index. Although the calculation of each of the tables by the Tellus model can be rather time consuming in proportion to the accuracy required the search and interpolation operations are very fast and allow the use of the Tellus model with pixel by pixel input.



## 5 RESULTS - SOIL MOISTURE AND EVAPORATION MAPS

### 5.1 Simulated Night Temperatures

As already said, the process set up here uses a series of look-up tables generated by the Tellus model. For each table, Tellus simulates Td and Tn values which must fit with the various input parameters (weather data, albedo, etc.) and with a set of values of THI and RSH. In order to save computing time in the calculation of the 57 necessary tables, a fast version of the Tellus model was run which uses a somewhat high heat capacity to allow calculation time steps of one hour (instead of 2 to 5 minutes for the slow version which requires 5 minutes machine time per table). As a result, the simulated Tn values are systematically lower by about 1.5°. A second systematic error was produced by the very low wind speed during the night; earlier experiments showed that the simulated Tn falls below measured values by about 1° in this situation. The solution was to increase the simulated Tn values by 2.5°.

### 5.2 Thermal Inertia and Soil Moisture

The results were mapped for the fields for which Tellus was assumed applicable (Figs. 8 to 11 and Figs. 12 to 16). Vegetated zones like meadows, forests, and standing cereal crops were not considered.

Figure 15 is the display of both thermal inertia and soil moisture mapped in 6 classes of thermal inertia/soil moisture. The soil moisture measurements available for our purpose were done only in the ploughed field and gave a mean value of 0.30 ($\sigma = \pm 0.024$) water content by weight determined over 8 core samples taken at 15 cm depth. The mean value of soil moisture calculated by Tellus over the whole field is 0.22 ± 0.03 by volume which corresponds to 0.21 ± 0.02 by weight, assuming a density of 1.1 gm $cm^{-3}$ for the 15 cm top soil layer. The calculated value is 30% lower but this comparison, although it is indicative for a tendency, should be considered with some caution; first because the moisture content of the core sample at 15 cm depth is not likely to be identical to the moisture content of the 15 cm top layer, second because the correspondence between thermal inertia and soil moisture leaves the depth of the top layer concerned somewhat undetermined and third because the top layer density is not known exactly and could vary from 1.0 to 1.2 gm $cm^{-3}$.

A comparison was made with apparent thermal inertia P calculated with the NASA-HCMM formula (NASA, 1978), expressed as $P = C(1 - a)/(Td - Tn)$, where a is the albedo and C is a constant which, in the present case, has been determined to fit with the mean values for the ploughed field of Td, Tn and THI calculated by Tellus. The results are displayed in Figure 13 with class limits identical to those used in Figure 15. As expected, the mapping inside the ploughed field is almost identical in the two figures. One can see that the general trends are roughly the same in the other fields. The detailed variations differ noticeably however, although to a minor degree for the fields towards the left side.

Further investigations should consequently examine the possibility to approximate the Tellus model with the help of such a simple formulation under well controlled and well calibrated conditions.

## 5.3 Cumulative Daily Evaporation

The mapped results obtained with Tellus are displayed in Figure 14. It is seen that CDE varies roughly in the same direction as THI and soil moisture which is reasonable. The detailed behaviour of CDE is however more complex because of the role played by RSH in the look-up tables. Two fields have for instance higher mean values of CDE than the three fields located between them (towards the left side of Figure 14), although having about the same average THI value as the latter; this is due to much higher RSH values, on the average, for the two fields.

Evaporation is estimated to be zero (or negative, which means condensation) for 0% of the total area. As condensation did not actually occur during the flight experiment, one must conclude that low range evaporation is not estimated well by the model.

Limiting values of CDE have been calculated with the Tergra model (Soer, 1980) for a volume moisture content of 0.44 (i.e. THI = 1940) and RSH = 1.0; they are compared in Table 21 to the Tellus values, which are lower by about 10%.

TABLE 21 CUMULATIVE DAILY EVAPORATION CALCULATED BY TERGRA AND TELL-US MODELS FOR VOLUME MOISTURE CONTENT 0.44 AND RELATIVE SURFACE HUMIDITY 1.0

| Aer. Roughness (m) | ALBEDO | CDE Tergra (mm) | CDE Tell-us (mm) | Difference % |
|---|---|---|---|---|
| 0.010 | 0.07 | 2.30 | 2.07 | 10 |
| 0.020 | 0.07 | 2.45 | 2.29 | 7 |
| 0.010 | 0.14 | 2.12 | 1.85 | 13 |
| 0.020 | 0.14 | 2.29 | 2.06 | 10 |

# 6 CONCLUSIONS

Several conclusions may be drawn from the 1977 Joint Flight Experiment but perhaps the most important factor is that it happened when it did, at the start of a large international experiment using a type of data unfamiliar to many of the partici-



pants. Many of the mistakes could be made early, experience could be pooled, and a data set made early to allow work to proceed. It is recommended that similar flight experiments be done on all future international remote sensing projects in Europe. The results from the experiments enabled the energy balance models to be tested, the registration procedures to be tested satisfactorily and the various atmospheric and radiometric correction methods to be tried. It was shown that it is possible to produce maps of both evaporation and soil moisture, with acceptable accuracy, at least for relative purposes. Further work on reducing the complexity of the procedures is required for operational purposes, but there is little doubt that an operational scheme is possible for irrigation scheduling, flood management and other uses.


## ACKNOWLEDGEMENTS

The United Kingdom Joint Flight Experiment was sponsored and funded by the Commission of the European Communities Joint Research Centre, Ispra, Varese, and the United Kingdom Natural Environment Research Council. Personnel from the Universities of Reading and Leeds took part in the data collection in addition to those from the Institute of Hydrology, a component Institute of the Natural Environment Research Council, and from the Joint Research Centre. Dr.R.J. Gurney completed the editing of this report while a National Academy of Sciences/National Research Council Resident Research Associate in the Hydrological Sciences Branch of the Earth Survey Applications Division, Goddard Space Flight Centre, Greenbelt, Maryland, U.S.A.


## REFERENCES


Gurney, R.J. and Templeman, R.F. Using Remotely Sensed Data on a Univac 1108 Computer, Computer Applications, in press.

Maracci, G. and Sturm, B. (1975), Measurements of beam transmittance and path radiance for correcting Landsat data for solar and optical effects, Proc. 5th Conf. Space Optics, Marseille.

NASA (1978), Heat Capacity Mapping Mission (HCMM) Data Users' Handbook for Applications Explorer Mission - A (AEM), Goddard Space Flight Center, Greenbelt, Maryland.

Reiniger, P. (1978), United Kingdom Joint Flight Experiment Flight Report, Joint Research Center, Ispra, Varese.

Rogers, R.H., Peacock, K. and Shah, N.L. (1973), A technique for correcting ERTS data for solar and atmospheric effects, Third ERTS Symposium, Goddard Space Flight Center, Greenbelt, Maryland.

Rosema, A., Bijleveld, J.G., Reiniger, P., Tassone, G., Blyth, K., Gurney, R J. (1978), "Tellus", a Combined Surface Temperature, Soil Moisture and Evaporation Mapping Approach, 12th International Symposium on Remote Sensing of the Environment, Manila, Philippines.

Rosenfeld, A. and Kak, A.C. (1976), *Digital Picture Processing*, Academic Press, New York, pp xii + 457.

Selby, J.E.A. and McClatchey, R.A. (198 ), Atmospheric transmittance from 0.25 to 28.5 µm, Computer Code Lowtran 4, Air Force Cambridge Research Laboratory, Cambridge, Mass.

Soer, G.J.R. (1980), Estimation of Regional Evapotranspiration and Soil Moisture Conditions Using Remotely Senses Crop Surface Temperatures, *Remote Sensing of Environment*, 9, 27-45.

Turner, R.C. and Spencer, M. (1972), Atmospheric model for correction of spacecraft data, Proc. 8th Symp. on Remote Sensing of Environment, Ann Arbor, Michigan.